mathematics

Article

An Enhanced Slime Mould Optimizer That Uses Chaotic Behavior and an Elitist Group for Solving Engineering Problems

Shahenda Sarhan [1,2,*], Abdullah Mohamed Shaheen [3], Ragab A. El-Sehiemy [4] and Mona Gafar [5,6]

1 Faculty of Computing and Information Technology, King Abdulaziz University, Jeddah 21589, Saudi Arabia
2 Faculty of Computers and Information Sciences, Mansoura University, Mansoura 35516, Egypt
3 Department of Electrical Engineering, Faculty of Engineering, Suez University, Suez 43533, Egypt; abdullahshaheen2015@gmail.com
4 Department of Electrical Engineering, Faculty of Engineering, Kafrelsheikh University, Kafrelsheikh 33516, Egypt; elsehiemy@eng.kfs.edu.eg
5 Department of Computer Science, College of Science and Humanities in Al-Sulail, Prince Sattam Bin Abdulaziz University, Kharj 16278, Saudi Arabia; m.gafar@psau.edu.sa
6 Machine Learning and Information Retrieval Department, Artificial Intelligence, Kafrelsheikh University, Kafrelsheikh 33516, Egypt
* Correspondence: sssarhan@kau.edu.sa

Abstract: This article suggests a novel enhanced slime mould optimizer (ESMO) that incorporates a chaotic strategy and an elitist group for handling various mathematical optimization benchmark functions and engineering problems. In the newly suggested solver, a chaotic strategy was integrated into the movement updating rule of the basic SMO, whereas the exploitation mechanism was enhanced via searching around an elitist group instead of only the global best dependence. To handle the mathematical optimization problems, 13 benchmark functions were utilized. To handle the engineering optimization problems, the optimal power flow (OPF) was handled first, where three studied cases were considered. The suggested scheme was scrutinized on a typical IEEE test grid, and the simulation results were compared with the results given in the former publications and found to be competitive in terms of the quality of the solution. The suggested ESMO outperformed the basic SMO in terms of the convergence rate, standard deviation, and solution merit. Furthermore, a test was executed to authenticate the statistical efficacy of the suggested ESMO-inspired scheme. The suggested ESMO provided a robust and straightforward solution for the OPF problem under diverse goal functions. Furthermore, the combined heat and electrical power dispatch problem was handled by considering a large-scale test case of 84 diverse units. Similar findings were drawn, where the suggested ESMO showed high superiority compared with the basic SMO and other recent techniques in minimizing the total production costs of heat and electrical energies.

Keywords: slime mould optimizer; chaotic behavior; elitist group; optimal power flow; fuel costs; heat and electrical power dispatch problem

MSC: 68T20

check for updates

Citation: Sarhan, S.; Shaheen, A.M.; El-Sehiemy, R.A.; Gafar, M. An Enhanced Slime Mould Optimizer That Uses Chaotic Behavior and an Elitist Group for Solving Engineering Problems. *Mathematics* **2022**, *10*, 1991. https://doi.org/10.3390/math10121991

Academic Editor: Alessandro Niccolai

Received: 5 May 2022
Accepted: 25 May 2022
Published: 9 June 2022

1. Introduction

The term "optimization process" relates to the procedure of determining the optimal settings for certain system characteristics in order to complete the design, operation, or planning tasks at the lowest possible cost [1]. Practical implementations and issues in artificial intelligence and machine learning are, in general, unconstrained or discrete [2]. As a result, finding optimal alternatives using standard mathematically based programming approaches is difficult [3]. Therefore, numerous optimization techniques were created in recent years to enhance the efficiency of several systems and minimize computing costs. Conventional optimization techniques have several flaws and restrictions, such as convergence to local optima and an undefined search space. Furthermore, they only provide a single-based solution [4].

On the other hand, effective optimization techniques must be applied when solving real-world optimization problems. In electrical power systems, they are necessary for the effective integration [5], analysis, control, and administration of modern design network processes [6]. OPF is a multi-modal, non-linear, non-differentiable, non-convex, and constrained minimization problem that involves fulfilling a combination of operating, technological, and security constraints, as well as picking optimal control variable values. OPF aims to lower energy generation and distribution operating costs by controlling control variables while keeping economic, technical, and environmental considerations in view [7].

Moreover, from the perspective of economic and environmental conservation, the combined heat and electrical power dispatch (CHEPD) problem has piqued the attention of several scholars. Numerous approaches to the CHPED issue were developed over time, including computational approaches and meta-heuristic methods. Power plants of thermal nature use fossil fuels, such as gas, coal, or oil to generate electricity. During the production of electricity, high-temperature heat is used to create steam power. Despite this, low-temperature heat is wasted via cooling systems, flue gas, and other means. As a result, a thermal power plant's efficiency is reduced to 50 to 60%. However, during the heating process, several forms of pollution, such as sulfur, nitrogen, and carbon dioxide, are produced, causing the warming effect and harming the ecological landscape. Cogeneration systems where heat and power producers generate energy at the minimum potential costs while minimizing pollutants are referred to as combined heat and power economic dispatch (CHEPD) [8].

Meta-heuristic algorithms have received a lot of interest and have been used to manage a wide range of optimization issues. They have common aspects, including the search strategy, which comprises two stages [9], the first of which is termed diversification (exploration), and the second is called intensification (exploitation). The meta-heuristic method creates randomized operations in the first stage to investigate various searching space areas. The optimization approach then attempts to find the best solution in the searching area in the second stage. To prevent entrapment at an optimum, an efficient meta-heuristic optimization technique must strike a balance between the exploration and exploitation phases.

Physics-based algorithms, evolutionary algorithms, swarm intelligence algorithms, and human-based algorithms are the four main types of meta-heuristic algorithms. Physical rules, such as the Henry gas solubility algorithm [4] and equilibrium algorithm (EA) [10–13], motivate physics-based algorithms. Evolutionary algorithms were developed by modeling biological evolutionary characteristics, such as mutations, crossovers, and selections, as described in [14,15] regarding the genetic algorithm and in [16] regarding the evaluation strategy. Swarm intelligence algorithms, such as jellyfish search optimization (JFSO) [17], grasshopper optimization GO [18], JFSO [17], GO [18], heap-based technique (HT) [19], whale optimization algorithm (WOA) [20], manta rays foraging optimization (MRFO) [21], marine predators algorithm (MPA) [22], particle swarm optimization [23], and artificial bee colony [24], are a series of techniques influenced by swarming and animal group behavior.

A slime mould optimizer (SMO) is a novel technique that was developed by considering the spreading and foraging behavior of slime mould and presented in 2020 by Li et al. [25]. The basic SMO has a unique mathematical model and very competitive results, along with a simple code structure. The gradient-free SMO method simulates positive and negative feedbacks of the propagation wave of slime mould. It has been used to address various real engineering optimizing issues because of its high globally searching ability and resilience, such as economic emission dispatch [26], optimal power flow [27], operation of cascade hydropower stations [28], demand estimation of urban water resources [29], and design optimization problems [30]. Added to that, other recent versions of the SMO were effectively presented, such as the leader SMO (LSMO) [31], equilibrium SMO (EQSMO) [32], adaptive opposition SMO (AOSMO) [33], and fitness-distance-balance SMO (FDBSMO) [34]. Additionally, different statistical comparisons of the competing meta-heuristic optimization were reviewed [35,36], where numerous runs of different optimizers can be effectively compared. Both studies stated the importance of the statistical comparison of stochastic optimizations and displayed the significance of the Friedman ranking test, Wilcoxon rank-sum test, and the convergence rates in terms of the average, median, and best obtained results.

However, in the present period, SMO still has several drawbacks, such as low computation precision and a premature convergence rate on specific benchmark problems [29]. Hence, in this study, an enhanced slime mould optimizer (ESMO) that uses chaotic behavior and an elitist group was proposed for solving engineering problems. The proposed ESMO provided two modifications to the standard SMO to enhance its performance. At first, to enhance the exploitation searching feature, an elitist group was created and updated to store the best individuals in each iteration. Second, to enhance the exploration searching feature, a logistic map that uses chaotic behavior was designed to boost the searching in a highly stochastic nature. The main contributions proposed in this study are listed as follows:

- A chaotic logistic mapping and an elitist group were combined with SMO to formulate a novel ESMO with better performance.
- The standard SMO and the proposed ESMO were applied to several benchmark functions and different practical engineering problems, including the OPF in power systems and the CHEPD combined heat and power systems.
- When handling different uni-modal and multi-modal functions, the proposed ESMO provided better performance than the original SMO and miscellaneous recent algorithms.
- When handling the OPF, the proposed ESMO demonstrated superiority over several reported techniques in minimizing the fuel costs, the losses, and the pollutant emissions.
- When handling the CHEPD problem, the proposed ESMO achieved the minimum total production costs against several reported techniques
- Moreover, better robustness and stability were demonstrated by the proposed ESMO compared with different recent SMO versions.

2. Enhanced Slime Mould Optimizer

2.1. Standard Slime Mould Optimizer

The slime mould optimizer (SMO) is a novel optimizer that relies on the oscillation pattern of slime mould in reality. It has a distinctive computational framework that uses dynamic weights to imitate the processes to produce positive and negative responses of the slime mould propagation wave to constitute the optimized route for attaching food [25]. An initial SMO population of n individuals is used for every d-dimensional optimizing task. Equation (1) initializes each member in the population as a vector with d entries.

$$Y_j(0) = Y_{\min} + rand(0,1)\cdot[Y_{\max} - Y_{\min}] \quad j = 1:n \tag{1}$$

where $Y_{\min}$ and $Y_{\max}$ are the solutions representing the control variables' minimum and maximum bounds.

In the standard SMO, there are two stages, namely, the approach and food wrapping [37]. In the first stage, because slime mould may pursue food based on the scent in the air, this behavior can be represented using the formula below:

$$Y_j(It+1) = \begin{cases} Y_b(It) + v_1\cdot(W\cdot Y_{r_1}(It) - Y_{r_2}(It)) & \Pr > r \\ v_2\cdot Y_j(It) & \Pr \le r \end{cases} \quad j = 1:n \tag{2}$$

where It is the present iteration, Y_j is the slime mould position, Y_b is the position with the greatest odor concentration, and Y_{r1} and Y_{r2} are two solutions chosen at random from the population. The slime mould selection behavior is replicated by two components, namely, v_1 and v_2, where v_2 decreases linearly from 1 to 0. W is the weight of the search agent, while r is a random value between [0, 1]. The Pr formula is written as follows:

$$\mathrm{Pr} = \tanh|S(j) - OBF| \quad j = 1 : n \tag{3}$$

where *S*(*j*) denotes the present individual's fitness score and *OBF* denotes the overall best fitness score over all the iterations. The following is the formula for v_1:

$$v_1 = \left[-\mathrm{arctanh}\left(1 - \frac{2}{\max_{It}}\right), \mathrm{arctanh}\left(1 - \frac{2}{\max_{It}}\right)\right] \tag{4}$$

where the maximum number of iterations is represented by $\max_{It}$. The following is the weight *W* [38,39]:

$$W(Index_{smell}(j)) = \begin{cases} 1 + r\cdot \log\left(\frac{BF - S(j)}{BF - WF} + 1\right), & condition \\ 1 - r\cdot \log\left(\frac{BF - S(j)}{BF - WF} + 1\right), & others \end{cases} \quad j = 1 : n \tag{5}$$

Condition indicates the first half of the population and *r* is a randomized value within [0, 1]. The optimal and worst values acquired in the current iteration are denoted by *BF* and *WF*, respectively, and $Index_{smell}$ represents the sorted series of fitness ratings:

$$Index_{smell} = sort(S) \tag{6}$$

When searching, the second stage computationally models the contraction mechanism of slime mould's venous tissue arrangement. The slime mould may change the searching behaviors based on the food quality that it eats. The slime mould's exact model for adjusting its location is as follows:

$$Y_j(It + 1) = \begin{cases} Y_{\min} + rand(0, 1)\cdot[Y_{\max} - Y_{\min}] & rand < z \\ Y_b(It) + v_1\cdot(W\cdot Y_{r_1}(It) - Y_{r_2}(It)) & \mathrm{Pr} > r \\ v_2\cdot Y_j(It) & \mathrm{Pr} \leq r \end{cases} \tag{7}$$

where *rand* and *r* are randomized values within [0, 1]. *z* is a parameter that determines how well a balancing process can explore and utilize data, and distinct values may be used depending on the situation. Figure 1 explains the steps of the SMO.

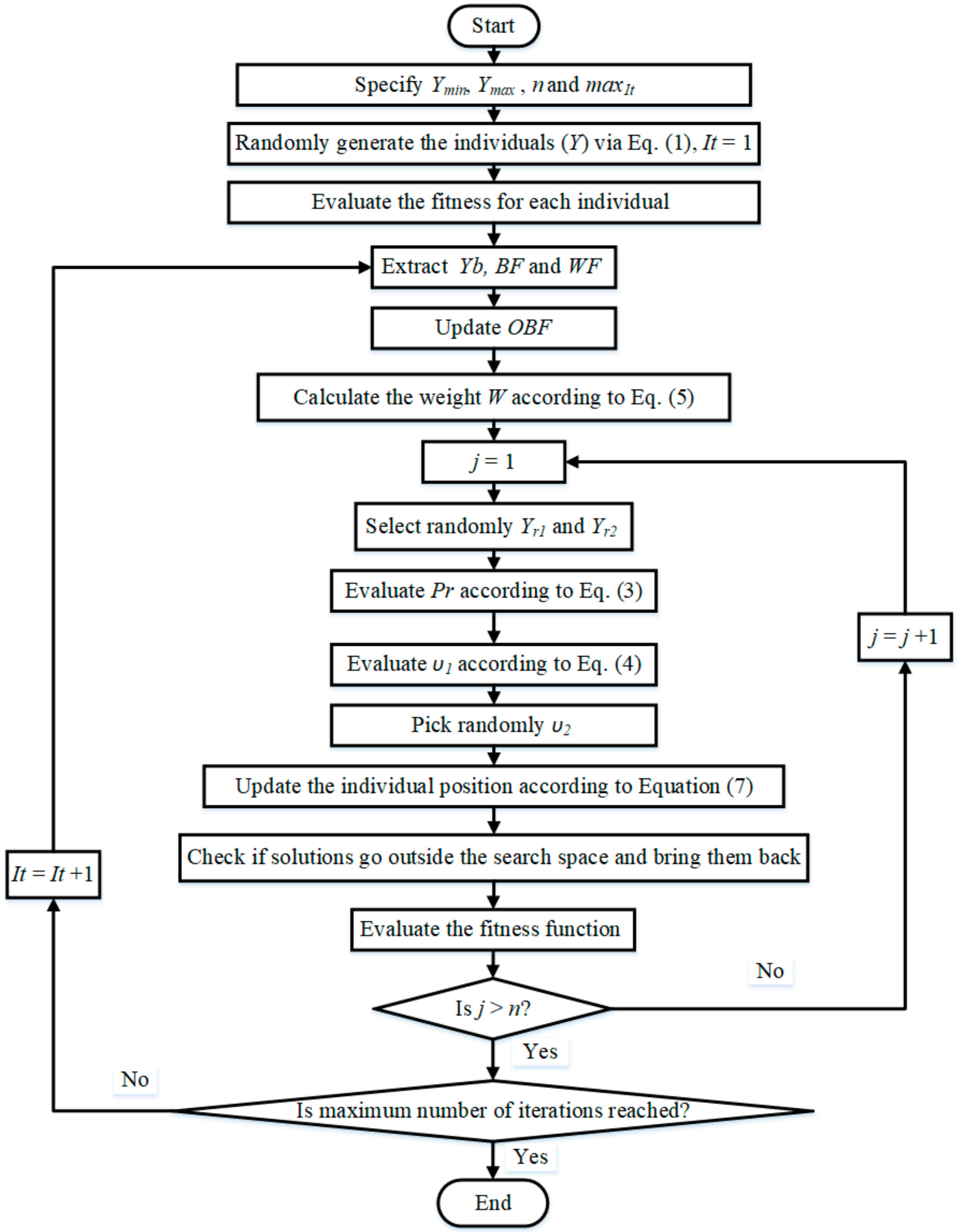

Figure 1. Flowchart of the SMO.

2.2. Proposed ESMO

In this section, an enhanced slime mould optimizer (ESMO) that uses chaotic behavior and an elitist group algorithm is presented to improve the performance of the standard SMO.

The SMO's performance is improved by two changes. To enhance the exploitation searching feature, an elitist group, with a size of five individuals, is created and updated to store the best four individuals in each iteration besides the mean individual, just like the equilibrium pool in EA [9], as follows:

$$Y_j(It+1) = Y_{Elitist}(It) + v_1 \cdot (W \cdot Y_{r_1}(It) - Y_{r_2}(It)) \;\; if \; \Pr > r \tag{8}$$

$$Y_{Elitist}(It) = rand\big([Y_{b1}; Y_{b2}; Y_{b3}; Y_{b4}; Y_{Avg}]\big) \tag{9}$$

where $Y_{Elitist}$ is the elitist group with a size of five individuals, Y_b is the position with the greatest odor concentrations, and Y_{Avg} is the mean position over the first four greatest concentrations. Therefore, the first four positions are stored in the elitist group besides the average position. In each iteration, the best four individuals are updated and the mean individual over them is calculated.

Based on this, exploitation searching is supported in various preferred directions. Furthermore, to enhance the exploration searching feature, a logistic map that uses chaotic behavior is designed to boost the searching in a highly stochastic nature [40]. Based on that, a produced vector (Cm) is created via the chaotic logistic map as follows:

$$Cm_j(It+1) = 4Cm_j(It)(Cm_j(It) - 1)) \tag{10}$$

$$Cm(0) = rand(1, \dim) \tag{11}$$

Using Equation (11), a vector is generated in each iteration for each dimensional variable, as described in Figure 2. As shown, a highly stochastic nature is provided using the utilized chaotic logistic map, which supports the exploration searching feature.

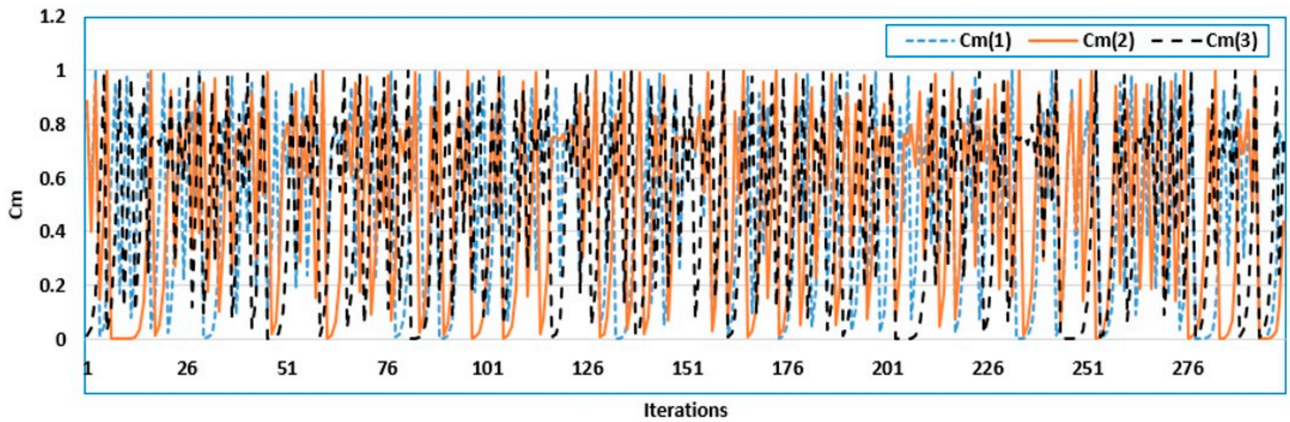

Figure 2. Logistic map based on chaotic behavior.

As a result, the standard SMO's updating process is adjusted, and the slime mould's new positions are adjusted as follows:

$$Y_j(It+1) = \begin{cases} Y_{\min} + rand(0,1) \cdot [Y_{\max} - Y_{\min}] & rand < z \\ Y_{Elitist}(It) + v_1 \cdot (W \cdot Y_{r_1}(It) - Y_{r_2}(It)) & \Pr > r \\ v_2 \cdot Cm_j \cdot Y_j(It) & \Pr \le r \end{cases} \tag{12}$$

Based on the chaotic behavior and elitist group algorithm, the proposed ESMO's main steps are depicted in Figure 3.

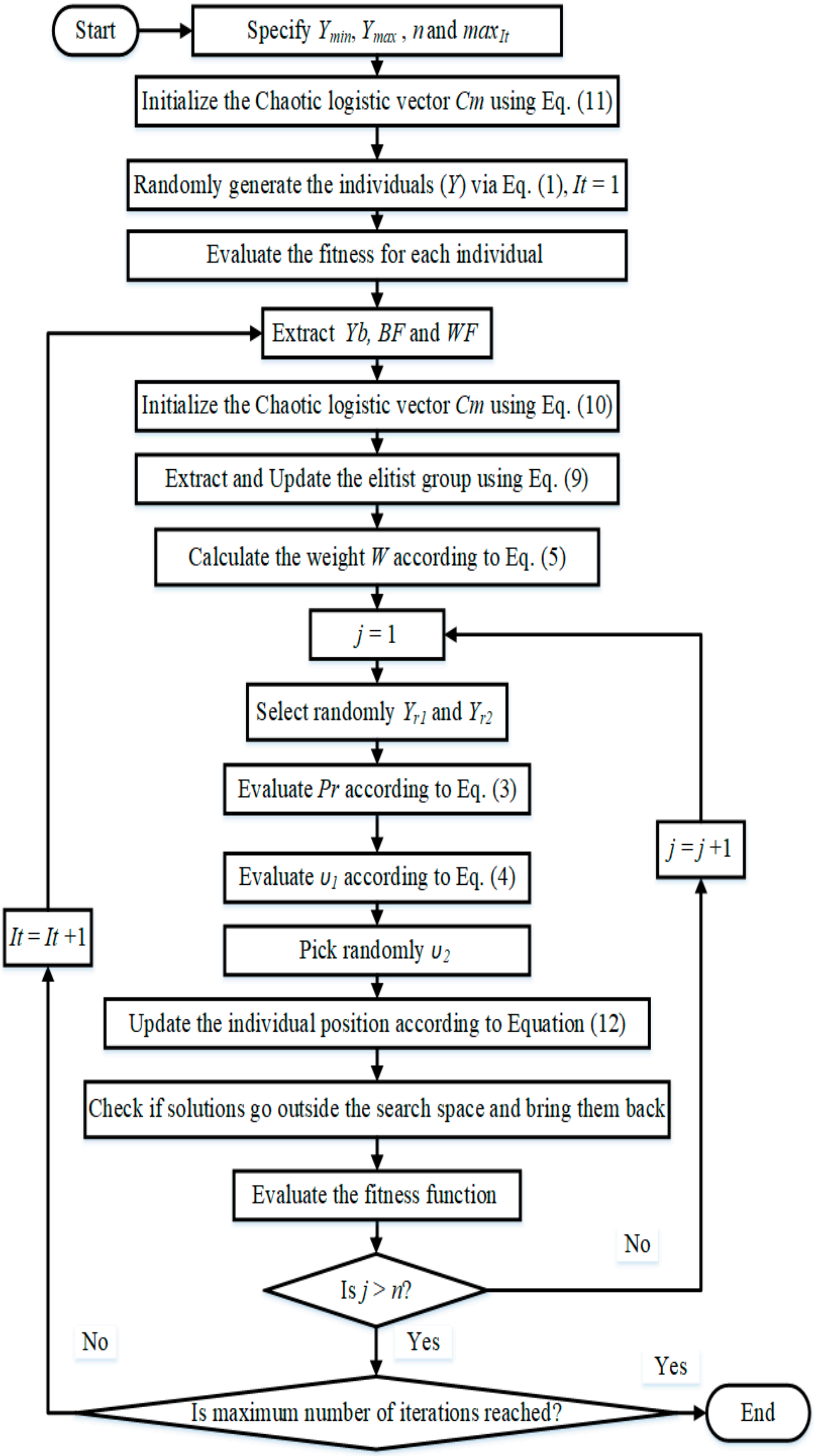

Figure 3. Proposed ESMO flowchart.

3. Application for Benchmark Optimization Functions

The results of the effectiveness and functionality evaluations of the suggested ESMO and SMO are presented in this section. They were examined using seven uni-modal and six multi-modal benchmark functions. Their detailed data are tabulated in Tables 1 and 2 in terms of their mathematical models, variable dimensions, and the considered ranges.

Table 1. Data of the tested uni-modal benchmark functions.

Function	Range	Dimension (d)	Minimum
$Fu_1 = \sum_{j=1}^{d} {x_j}^2$	[−100, 100]	30	0
$Fu_2 = \sum_{j=1}^{d} \lvert x_j \rvert + \Pi_{j=1}^{d} \lvert x_j \rvert$	[−10, 10]	30	0
$Fu_3 = \sum_{j=1}^{d} \left(\sum_{i-1}^{j} x_i \right)^2$	[−100, 100]	30	0
$Fu_4 = \max_j \left\{ \lvert x_j \rvert, 1 < j < d \right\}$	[−100, 100]	30	0
$Fu_5 = \sum_{j=1}^{d-1} \left[100(x_{j+1} - {x_j}^2) + (x_j - 1)^2 \right]$	[−30, 30]	30	0
$Fu_6 = \sum_{j=1}^{d} \left(\left[x_j + 0.5 \right] \right)^2$	[−100, 100]	30	0
$Fu_7 = \sum_{j=1}^{d} j{x_j}^4 + random[0,1]$	[−128, 128]	30	0

Table 2. Data of the tested multi-modal benchmark functions.

Function	Range	d	Min.
$Fm_1 = \sum_{j=1}^{d} \left(-x_j \sin(\sqrt{\lvert x_j \rvert}) \right)$	[−500, 500]	30	−418.9829 × d
$Fm_2 = \sum_{j=1}^{d} \left({x_j}^2 - 10\cos(2\pi x_j) + 10 \right)$	[−5.12, 5.12]	30	0
$Fm_3 = -20\exp\left(-0.2 \left(\frac{1}{d} \sum_{j=1}^{d} {x_j}^2 \right)^{\frac{1}{2}} \right) - \exp\left(\frac{1}{d} \sum_{j=1}^{d} \cos(2\pi x_j) \right) + 20 + e$	[−32, 32]	30	0
$Fm_4 = \frac{1}{4000} \sum_{j=1}^{d} {x_j}^2 - \Pi_{j=1}^{d} \cos\left(\frac{x_j}{\sqrt{j}} \right) + 1$	[−600, 600]	30	0
$Fm_5 = \frac{\pi}{d} 10\sin(\pi z_1) + \sum_{j=1}^{d-1} \left[(z_j - 1)^2 \left(1 + 10\sin^2(\pi z_{j+1}) \right) \right]$ $+ (z_d - 1)^2 + \sum_{j=1}^{d} u\left(x_j, 10, 100, 4 \right)$ $where, z_j = \frac{1+x_j}{4} + 1, u(x_j, \alpha, \beta, \gamma) = \begin{cases} \beta(x_j - \alpha)^\gamma & if\ x_j > \alpha \\ 0 & if\ -a < x_j < \alpha \\ \beta(-x_j - \alpha)^\gamma & if\ x_j < \alpha \end{cases}$	[−50, 50]	30	0
$Fm_6 = 0.1 \left(\begin{array}{c} \sum_{j=1}^{d} (x_j - 1)^2 \left[1 + \sin^2(3\pi x_j + 1) \right] \\ + \sin^2(3\pi x_1) + (x_d - 1)^2 [1 + \sin^2(3\pi x_d)] \end{array} \right) + \sum_{j=1}^{d} u\left(x_j, 5, 100, 4 \right)$	[−50, 50]	30	0

The suggested ESMO were assessed in comparison to the standard SMO, sine cosine algorithm (SCA) [41], salp swarm algorithm (SSA) [42], whale optimization algorithm (WOA) [20], multiverse optimizer (MVO) [43], PSO [44], and DE [45], as depicted in [25]. The parameters were chosen depending on those employed by the original source in the study or those generally utilized by other researchers. The detailed data of the parameter settings of these implemented techniques are described in Appendix A (Table A1).

To ensure fairness and consistency during the comparison, the methods were run under similar conditions. The numbers of solution individuals and iterations were assigned to be 30 and 1000, respectively. To minimize the effects of randomness in the algorithms, thirty run times were considered for each function and the mean outcome was used. The means, standard deviations (STds), and medians were used to analyze the outcomes for the purpose of quantifying them. Their comparisons for uni-modal and multi-modal optimization functions are tabulated in Tables 3 and 4, respectively. As illustrated, the suggested ESMO had a stronger resilience in terms of obtaining the smallest mean, STd and median in more than 50% of benchmark functions. For uni-modal functions, the suggested ESMO always provided the capability to find the minimum median fitnesses of 0, 0, 0, 0, 0.057554, 0.000436, and 5.98×10^{-5}, respectively, for the seven tested functions. Furthermore, it showed great performance in terms of the means and STds compared with SMO, SCA, SSA, WOA, MVO, PSO, and DE. Similar findings were obtained for the multi-modal benchmark functions. The suggested ESMO always provided the capability to find the minimum median fitnesses of −12,569.5, 0, 8.88×10^{-16}, 0, 0.000204, and 0.00047, respectively, for the six tested functions, with great performance in terms of the means and STds compared with the others.

Table 3. Comparisons of the mean, STd, and median fitnesses for the uni-modal benchmark functions.

Function	Index	ESMO	SMO	SCA	SSA	WOA	MVO	PSO	DE
Fu_1	Mean	0	0	0.015244	1.23×10^{-8}	4.32×10^{-153}	0.318998	128.8037	3.03×10^{-12}
	STd	0	0	0.029989	3.54×10^{-9}	2.28×10^{-152}	0.11206	15.36838	3.45×10^{-12}
	Median	0	1.08×10^{-64}	93.6	183	2.34×10^{-54}	940	142	0.000401
Fu_2	Mean	0	5.33×10^{-207}	1.15×10^{-5}	0.848146	5.03×10^{-104}	0.38893	86.07543	3.72×10^{-8}
	STd	0	0	2.74×10^{-5}	0.941518	1.59×10^{-103}	0.137834	65.29881	1.2×10^{-8}
	Median	0	5.93×10^{-58}	0.00806	8.9	3.42×10^{-34}	13.9	112	0.00224
Fu_3	Mean	0	0	3261.997	236.6219	20,802.28	48.11246	406.9626	24,230.57
	STd	0	0	2935.038	155.5471	10,554.39	21.77526	71.30926	4174.379
	Median	0	0.0822	27,500	2940	53,000	4610	606	30,000
Fu_4	Mean	0	2.30×10^{-197}	20.53249	8.254602	45.70634	1.076968	4.498158	1.965929
	STd	0	0	11.04664	3.287966	26.93504	0.310884	0.329339	0.430531
	Median	0	1.31×10^{-25}	75.3	16.2	46.1	14	4.79	13.2
Fu_5	Mean	2.286848	0.42779	532.7126	135.5698	27.26543	407.9465	154736	46.12942
	STd	6.936666	0.637	1907.446	174.1213	0.57447	615.329	36,039	27.29727
	Median	0.057554	9.89	1,580,000	7770	27.3	86,300	185,000	140
Fu_6	Mean	0.000477	0.000879	4.550121	0	0.100557	0.323756	132.779	3.1×10^{-12}
	STd	0.000281	0.000415	0.357049	0	0.110525	0.097394	15.189	1.46×10^{-12}
	Median	0.000436	0.597	33.7	204	0.101	934	145	0.000411
Fu_7	Mean	7×10^{-5}	8.84×10^{-5}	0.024382	0.095541	0.000986	0.020859	111.0068	0.026937
	STd	6.31×10^{-5}	7.12×10^{-5}	0.020732	0.05053	0.001147	0.009584	21.5378	0.006322
	Median	5.98×10^{-5}	0.000408	0.604	0.159	0.00266	0.142	111	0.0544

Table 4. Comparisons of the mean, STd and median fitnesses for the multi-modal benchmark functions.

Function	Index	ESMO	SMO	SCA	SSA	WOA	MVO	PSO	DE
Fm_1	Mean	−12,569.5	−12,569.4	−3886.1	−7816.8	−11,630.6	−7744.9	−6728.1	−12,409.8
	STd	0.018169	0.1	225.6	842.3	1277.5	693.4	650.2	149.2
	Median	−12,569.5	−12,600	−3820	−6980	−11,500	−5590	−6720	−9930
Fm_2	Mean	0	0	18.35521	56.61307	0	112.7184	369.2446	59.28367
	STd	0	0	21.43693	12.89967	0	24.57189	18.68261	6.07679
	Median	0	0.996	72.2	138	0	233	373	86
Fm_3	Mean	8.88×10^{-16}	8.88×10^{-16}	11.32308	2.25688	3.97×10^{-15}	1.14572	8.41508	4.64×10^{-7}
	STd	0	0	9.66101	0.72068	2.03×10^{-15}	0.70341	0.41051	1.38×10^{-7}
	Median	8.88×10^{-16}	8.88×10^{-16}	14.2	5.03	4.09×10^{-15}	7.7	8.75	0.00566
Fm_4	Mean	0	0	0.23534	0.01009	0	0.57543	1.03228	9.76×10^{-11}
	STd	0	0	0.2248	0.01067	0	0.08747	0.00489	2.13×10^{-10}
	Median	0	0	1.29	2.75	0	8.98	1.04	0.00756
Fm_5	Mean	0.000813	0.001195	2.290194	5.542545	0.005205	1.294524	4.80322	3.63×10^{-13}
	STd	0.001482	0.001422	2.958865	3.122247	0.003512	1.103471	0.8667	3.4×10^{-13}
	Median	0.000204	0.0142	34,800,000	21.7	0.00521	12.7	5.16	5.03×10^{-5}
Fm_6	Mean	0.001589	0.001577	518.6869	1.010473	0.181197	0.081286	23.19158	1.69×10^{-12}
	STd	0.003359	0.003	2782.845	4.701096	0.166955	0.043182	4.195613	1.16×10^{-12}
	Median	0.00047	0.145	17,800,000	95.1	0.181	1780	28.8	0.000244

Additionally, a Friedman ranking test of the mean obtained fitness was executed for the uni-modal and multi-modal benchmark functions for the suggested ESMO, SMO, SCA, SSA, WOA, MVO, PSO, and DE, as depicted in Table 5.

Table 5. Friedman ranking test results of the mean obtained fitness for the uni-modal and multi-modal benchmark functions.

Function	ESMO	SMO	SCA	SSA	WOA	MVO	PSO	DE
Fu_1	1.5	1.5	5	4	7	6	8	3
Fu_2	1	2	4	6	7	5	8	3
Fu_3	1.5	1.5	6	4	7	3	5	8
Fu_4	1	2	7	6	8	3	5	4
Fu_5	2	1	7	5	3	6	8	4
Fu_6	3	4	7	1	5	6	8	2
Fu_7	1	2	5	7	3	4	8	6
Fm_1	2	1	8	5	4	6	7	3
Fm_2	1.5	1.5	4	5	1.5	7	8	6
Fm_3	1.5	1.5	8	6	3	5	7	4
Fm_4	1.5	1.5	6	5	1.5	7	8	4
Fm_5	2	3	6	8	4	5	7	1
Fm_6	3	2	8	6	5	4	7	1
Summation	22.5	24.5	81	68	59	67	94	49
Mean rank	1.6071429	1.75	5.7857143	4.8571429	4.2142857	4.7857143	6.7142857	3.5
Final Ranking	1	2	7	6	4	5	8	3

As shown, the suggested ESMO had higher robustness, as it occupied the first rank, with a mean rank of 1.607. On the other hand, the standard SMO occupied the second rank, with a mean rank of 1.75. In ascending order, the other algorithms were DE, WOA, MVO, SSA, SCA, and PSO, with mean ranks of 3.5, 4.2142857, 4.7857143, 4.8571429, 5.7857143, and 6.7142857, respectively.

4. Application for Engineering Optimization Problems

4.1. Optimal Power Flow in Electric Power Systems

Regarding the OPF issue, the control variables can be seen as follows:

- ($Pgen_1$, $Pgen_2$, … , $Pgen_{Ngen}$) denote the active output powers of the generators.
- ($Qcap_1$, $Qcap_2$, … , $Qcap_{Nq}$) denote the absorbing or injecting reactive powers via switched reactors and capacitors, respectively.
- ($Vgen_1$, $Vgen_2$, … , $Vgen_{Ngen}$) denote the generator voltages.
- (Ta_1, Ta_2, … , Ta_{Nt}) denote the transformer tap settings.

where N_{gen}, N_q, and N_t reflect the number of generators, reactive power sources, and tap changers, respectively.

Additionally, the dependent variables can be seen as follows:

- ($VLoad_1$, … , $VLoad_{NPQ}$) denote the load bus voltage magnitudes.
- ($Qgen_1$, $Qgen_2$, … , $Qgen_{Ngen}$) denote the reactive power of the generators.
- (S_1, … , S_{NF}) denote the transmission line loadings.

4.1.1. Minimization of the Fuel Costs

The OPF problem can be mathematically solved to minimize the fuel generation costs ($F1$), as described in Equation (13):

$$F1 = \sum_{k=1}^{Ng} a_k {Pgen_k}^2 + b_k Pgen_k + c_k \quad (13)$$

where a_k, b_k, and c_k are the cost coefficients of the generator k.

This minimization target should be handled by maintaining different equality constraints, as described in Equations (14)–(20), and inequality constraints, as described in Equations (21) and (22).

$$Pgen_k^{\min} \leq Pgen_k \leq Pgen_k^{max}, \ k = 1 : Ngen \tag{14}$$

$$Vgen_k^{\min} \leq Vgen_k \leq Vgen_k^{max}, \ k = 1 : Ngen \tag{15}$$

$$Qgen_k^{\min} \leq Qgen_k \leq Qgen_k^{max}, \ k = 1 : Ngen \tag{16}$$

$$Ta_L^{\min} \leq Ta_L \leq Ta_L^{max}, \ L = 1 : Nt \tag{17}$$

$$Qcap_{var}^{max} \leq Qcap_{var} \leq Qcap_{var}^{max}, \ var = 1 : Nq \tag{18}$$

$$VLoad_j^{\min} \leq VLoad_j \leq VLoad_j^{max}, \ j = 1 : NPQ \tag{19}$$

$$|S_{Line}| \leq S_{Line}^{max}, \ Line = 1 : Nf \tag{20}$$

$$Pgen_k - PLoad_k - V_k \sum_{j=1}^{Nb} V_j (G_{kj} \cos\theta_{kj} + B_{kj} \sin\theta_{kj}) = 0, \ k = 1 : Nb \tag{21}$$

$$Qgen_k - QLoad_k + Qcap_k - V_k \sum_{j=1}^{Nb} V_j (G_{kj} \sin\theta_{kj} - B_{kj} \cos\theta_{kj}) = 0, \ k = 1 : Nb \tag{22}$$

where *PLoad* and *QLoad* denote the active and reactive power demands, respectively; θ_{kj} is the phase angle difference between bus k and j; and B_{kj} is the mutual susceptance between bus k and j.

In the standard IEEE 30-bus system, the proposed ESMO and SMO were used. Thirty simulated tests were conducted for both the proposed ESMO and SMO, with a maximal number of iterations of 300 and a population number of 50. As illustrated in Figure 4, the basic IEEE 30-bus system consisted of 30 buses, 4 on-load tap changers, 9 capacitive sources, 6 generators, and 41 lines. The statistics for the allowable boundaries of reactive power production, buses, and transmission lines were derived from [46]. The allowable generator voltages were 1.1000 and 0.9500 p.u. for the minimum and maximum, respectively.

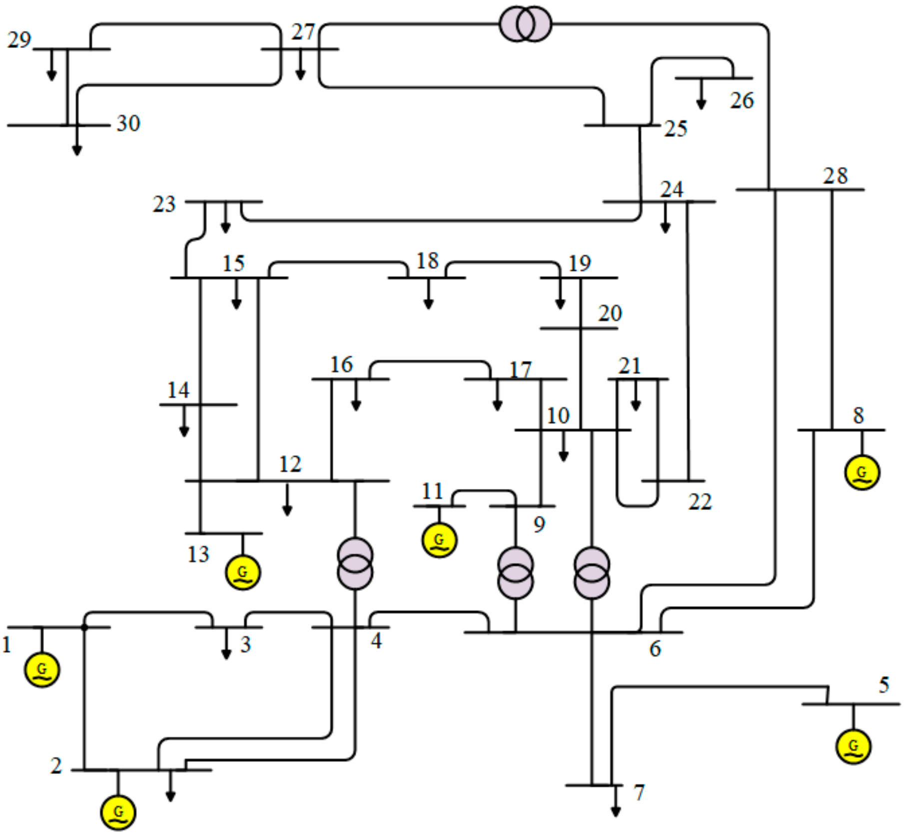

Figure 4. IEEE 30-bus system [47,48].

To minimize the fuel costs case, the proposed ESMO, standard SMO, and other recent versions of the SMO of LSMO [31], EQSMO [32], AOSMO [33], and FDBSMO [34] were performed. Table 6 describes the parameter settings of each applied algorithm to solve the OPF issue. As shown, the same number of function evaluations was maintained at 15,000 times and the same number of implementations was maintained at 30 times. These considerations guarantee a fair comparison with equivalent fitness functions between the applied methods.

Table 6. Parameter settings of the proposed ESMO and other recent SMO versions when minimizing the costs.

Variables	SMO	Proposed ESMO	LSMO [31]	EQSMO [32]	AOSMO [33]	FDBSMO [34]
Number of individuals	50	50	50	50	25	50
Number of iterations	300	300	300	300	300	300
Number of function evaluation per each individual	1	1	1	1	2	1
Total number of runs	30					
Total number of function evaluations	15,000					

The attained outputs of the proposed ESMO and other recent versions of the SMO, i.e., LSMO [31], EQSMO [32], AOSMO [33], and FDBSMO [34], are displayed in Table 7. In addition, Figure 5 depicts their average, median, and best convergence characteristics. The proposed ESMO clearly beat the other versions of the SMO in terms of reducing fuel costs. The proposed ESMO achieved the best value of 799.1134 USD/h, while the SMO achieved 799.202 USD/h vs. 901.96 USD/h in the initial condition. Furthermore, LSMO, EQSMO, AOSMO and FDBSMO achieved 799.2048692, 799.1730514, 799.1745189, and 799.12964 USD/h, respectively.

Table 7. Optimal results of the proposed ESMO and other recent SMO versions when minimizing the costs.

Variables	Initial	SMO	Proposed ESMO	LSMO	EQSMO	AOSMO	FDBSMO
$Vgen_{1}$	1.0500	1.099969602	1.1	1.1	1.1	1.1	1.1
$Vgen_{2}$	1.0400	1.088343999	1.087639528	1.088106605	1.088033924	1.087606497	1.087707536
$Vgen_{5}$	1.0100	1.061815867	1.061513432	1.062283384	1.062101361	1.061700294	1.060850352
$Vgen_{8}$	1.0100	1.069580017	1.070329805	1.070401666	1.069533777	1.069257672	1.06859214
$Vgen_{11}$	1.0500	1.099998144	1.1	1.1	1.1	1.099942632	1.1
$Vgen_{13}$	1.0500	1.1	1.1	1.1	1.1	1.1	1.1
$Ta_{6–9}$	1.0780	1.045635918	1.044369846	1.063643374	1.051376567	1.004989363	1.064422161
$Ta_{6–10}$	1.0690	0.931759565	0.911612439	0.9007877	0.929805666	0.974457082	0.9
$Ta_{4–12}$	1.0320	1.007802744	0.991122526	1.008046557	1.017551823	0.997683162	0.995096784
$Ta_{28–27}$	1.0680	0.971018798	0.964707994	0.963876332	0.979926365	0.977898669	0.972079256
$Qcap_{10}$	0	4.208618458	4.901566432	4.136822869	1.498053882	4.976971243	4.327592577
$Qcap_{12}$	0	1.451796819	4.383148586	4.94482842	0.696142216	4.884154333	4.667399693
$Qcap_{15}$	0	1.306875509	2.483268955	4.786681393	4.792743533	4.728549757	0.045181547
$Qcap_{17}$	0	5	4.998164786	2.130295748	5	4.958379139	4.998203992
$Qcap_{20}$	0	1.961100674	4.998940961	3.343858724	4.804278029	4.984821012	4.839667485
$Qcap_{21}$	0	4.803911173	4.984963132	4.602756718	5	4.602619108	4.998527988
$Qcap_{23}$	0	4.967076344	4.929896773	1.465312443	1.168975994	4.626528243	3.897113281
$Qcap_{24}$	0	4.996077919	5	4.836618584	4.927208177	4.641278115	5
$Qcap_{29}$	0	0.669299515	2.003815544	0.086094576	1.751011024	4.731956237	2.870308756
$Pgen_{1}$	99.2400	177.0369	177.054	177.4292091	177.0980781	177.3830955	177.2475961
$Pgen_{2}$	80	48.6588889	48.54725268	48.33560014	48.51216059	48.69172993	48.5077348
$Pgen_{5}$	50	21.33672043	21.38583045	21.2845056	21.22712818	21.3520339	21.23838842
$Pgen_{8}$	20	21.16227193	21.36222862	21.43941889	21.03134239	20.61578115	21.13968009
$Pgen_{11}$	20	11.9200414	11.93816688	11.58454651	12.18081624	11.95169297	11.91470514
$Pgen_{13}$	20	12.01013994	12.00255919	12	12	12.08219303	12.00039502
F1	901.9600	799.202	799.1134	799.2048692	799.1730514	799.1745189	799.12964

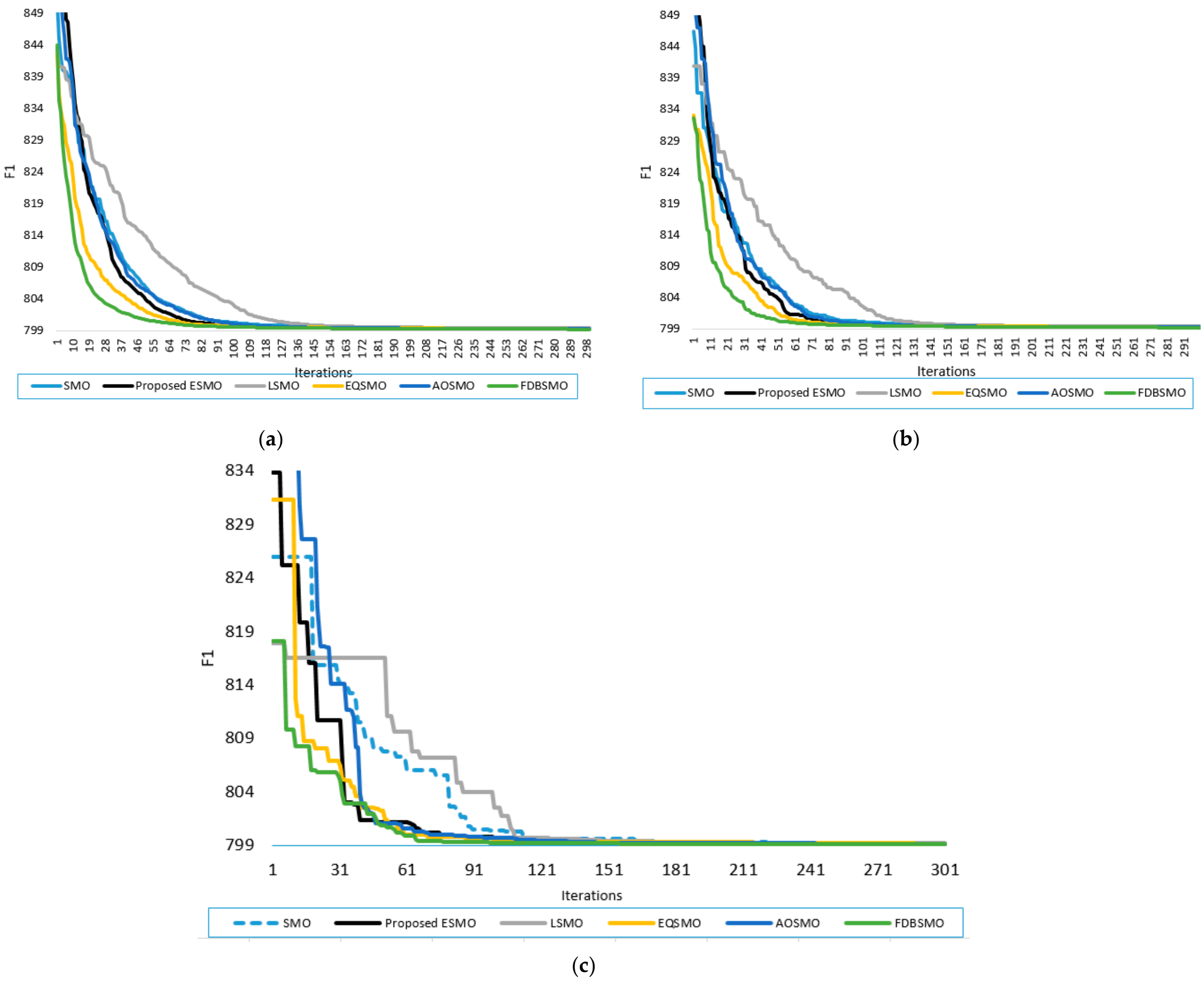

Figure 5. Convergences of the proposed ESMO and other SMO versions when minimizing the costs. (**a**) Average convergence; (**b**) Median convergence; (**c**) Best convergence.

In particular, after utilizing the suggested ESMO and other SMO versions, Figure 6 depicts the box plot of the thirty obtained fitnesses of the derived fuel costs. As shown, the suggested ESMO was effective at producing the lowest fuel cost values. In terms of the mean fuel costs, the suggested ESMO achieved a value of 799.2483 USD/h, whereas the SMO obtained a value of 799.437 USD/h. In terms of the maximum fuel costs, the suggested ESMO achieved a value of 799.2483 USD/h, whereas the SMO obtained a value of 799.5056 USD/h. Moreover, the ESMO provided a lower STd of 0.074835 compared with 0.085524 for the SMO.

In addition, Table 8 compares the outcomes of reducing the FCs (case 1) with numerous different methods, including MCSO [49], improved electromagnetism-like algorithm (IEOA) [50], NBO [51], CSO [52], black-hole-based optimization approach (BHBOA) [53], adaptive GO (AGO) [54], improved moth–flame optimization (IMFO) [55], teaching–learning algorithm (TLA) [56], developed grey wolf algorithm (DGWA) [57], moth swarm algorithm (MSA) [58], grasshopper optimizer (GO) [54], symbiotic organisms search (SOS) [59], imperialist competitive algorithm (ICA) [60], differential harmony search algorithm (DHSA) [61], and GA [62]. As shown, the proposed ESMO and the SMO obtained minimum fuel costs of 799.1134 USD/h and 799.202 USD/h, respectively, which were lower than the other techniques.

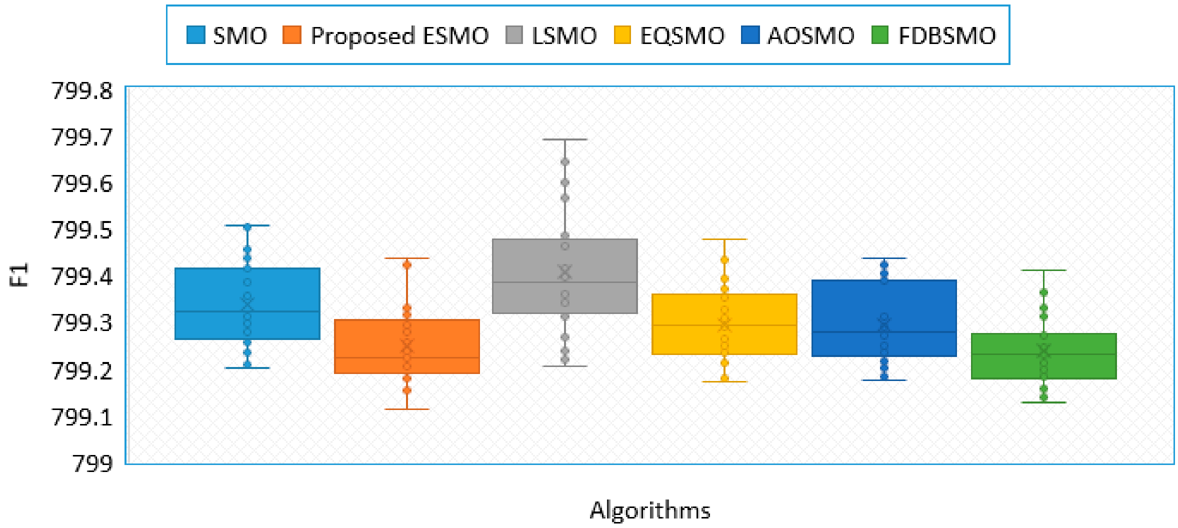

Figure 6. Box plot of the acquired fuel costs via the proposed ESMO and other SMO versions.

Table 8. Comparisons of the ESMO and other reported algorithms after minimizing the costs.

Method	F1
Proposed ESMO	799.1134
SMO	799.202
LSMO	799.2048692
EQSMO	799.1730514
AOSMO	799.1745189
FDBSMO	799.12964
MCSO [49]	799.3332
IEOA [50]	799.688
NBO [51]	799.7516
CSO [52]	799.8266
BHBOA [53]	799.9217
AGO [54]	800.0212
IMFO [55]	800.3848
TLA [56]	800.4212
DGWA [57]	800.433
MSA [58]	800.5099
GO [54]	800.9728
SOS [59]	801.5733
ICA [60]	801.843
DHSA [53]	802.2966
GA [62]	802.1962

4.1.2. Minimization of the Power Losses

Based on the preferences of power system operators, the OPF problem can be mathematically solved to minimize the power losses ($F2$), as described in Equation (23) [63]:

$$GLs = \sum_{k=1}^{Nb} \sum_{j=1}^{Nb} G_{kj}\left({V_k}^2 + {V_j}^2 - 2\left(V_k V_j \cos\theta_{kj}\right)\right) \tag{23}$$

where G_{kj} indicates the conductance of the line connected between buses k and j.

To minimize the power losses, the proposed ESMO and other SMO versions were performed, and their attained outputs are displayed in Table 9. In addition, Figure 7 depicts the convergence characteristics of the suggested ESMO and other SMO versions. The proposed ESMO clearly beat the other SMO versions in terms of reducing the power losses, as the proposed ESMO achieved the lowest value of 2.852 MW vs. 5.83 MW in the initial condition. Furthermore, the SMO, LSMO, EQSMO, AOSMO, and FDBSMO achieved 2.873, 2.8789, 2.87089, 2.869748, and 2.86545 MW, respectively. In particular, after utilizing the suggested ESMO and other SMO versions, Figure 8 depicts the box plot of the thirty obtained fitnesses of the derived power losses.

Table 9. Optimal results of the proposed ESMO and other recent SMO versions when minimizing the losses.

Variables	Initial	SMO	Proposed ESMO	LSMO	EQSMO	AOSMO	FDBSMO
Vgen $_{1}$	1.0500	1.1	1.1	1.1	1.1	1.1	1.099989573
Vgen $_{2}$	1.0400	1.097879	1.098038	1.097501943	1.096319677	1.097285716	1.09804085
Vgen $_{5}$	1.0100	1.079229	1.080119	1.079199519	1.080009144	1.078852719	1.081198314
Vgen $_{8}$	1.0100	1.088195	1.087402	1.087596906	1.08475669	1.087053678	1.088314909
Vgen $_{11}$	1.0500	1.1	1.099767	1.098598489	1.099455244	1.1	1.1
Vgen $_{13}$	1.0500	1.099676	1.1	1.1	1.1	1.1	1.1
Ta $_{6–9}$	1.0780	1.063533	1.070752	1.049470818	1.065452822	1.07056185	1.030097886
Ta $_{6–10}$	1.0690	0.905539	0.9	0.915931488	0.905932713	0.902753197	0.936000592
Ta $_{4–12}$	1.0320	0.985392	0.989256	1.000010356	0.985437987	0.992873237	0.987993017
Ta $_{28–27}$	1.0680	0.978031	0.973971	0.9844877	0.970903402	0.978152907	0.974034656
Qcap $_{10}$	0	4.977853	4.9364	2.838936239	4.993922257	3.950366074	0.706305597
Qcap $_{12}$	0	1.455635	4.832076	4.97359854	0.889625335	1.660906262	4.999986635
Qcap $_{15}$	0	1.525858	5	1.020706924	3.062849892	4.649982156	4.118956228
Qcap $_{17}$	0	3.578362	4.996391	4.525460006	4.999200578	4.650398836	4.986290979
Qcap $_{20}$	0	4.680336	4.706986	3.43393887	4.834020113	5	3.660338716
Qcap $_{21}$	0	4.99174	5	3.172761986	4.991919357	4.996140588	4.999935911
Qcap $_{23}$	0	3.525662	2.901574	4.355145722	2.759336009	4.962344585	4.11599159
Qcap $_{24}$	0	4.865855	4.973277	4.974977192	4.843678606	4.702638138	5
Qcap $_{29}$	0	1.472307	2.171079	2.732949574	0.863015243	3.022489789	2.035194665
Pgen $_{1}$	99.2400	51.33	51.26	51.29182179	51.27089863	51.2719091	51.28320001
Pgen $_{2}$	80	79.93523	79.99628	80	80	79.9978392	79.9824479
Pgen $_{5}$	50	50	50	50	50	50	50
Pgen $_{8}$	20	35	35	35	35	35	35
Pgen $_{11}$	20	30	30	29.99833311	30	30	29.99994255
Pgen $_{13}$	20	40	40	39.98873995	40	40	39.99986133
F2	5.832400	2.873533	2.852083	2.87889486	2.870898634	2.869748299	2.865451787

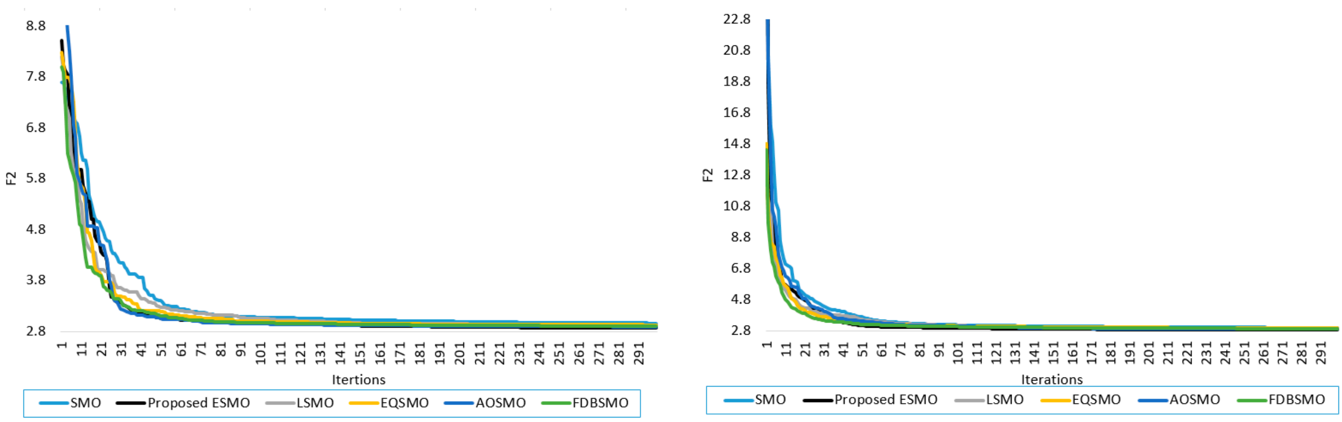

(a) (b)

Figure 7. *Cont.*

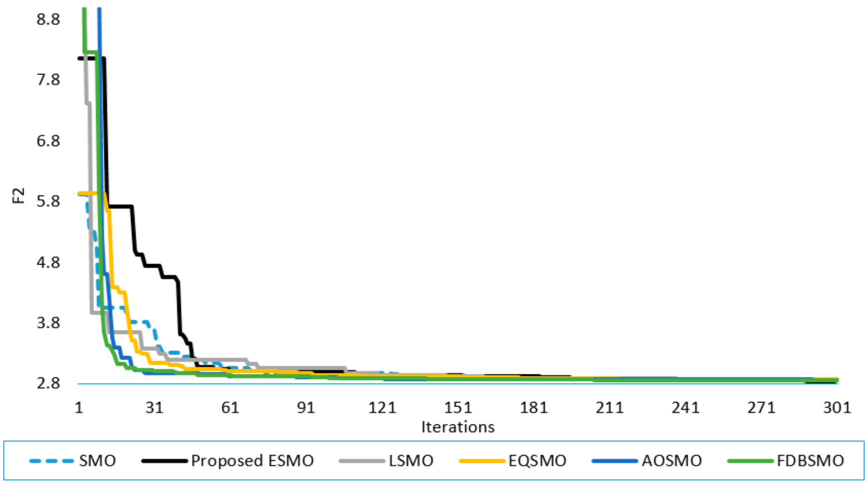

(**c**)

Figure 7. Convergences of the proposed ESMO and other recent SMO versions when minimizing the losses. (**a**) Average convergence; (**b**) Median convergence; (**c**) Best convergence.

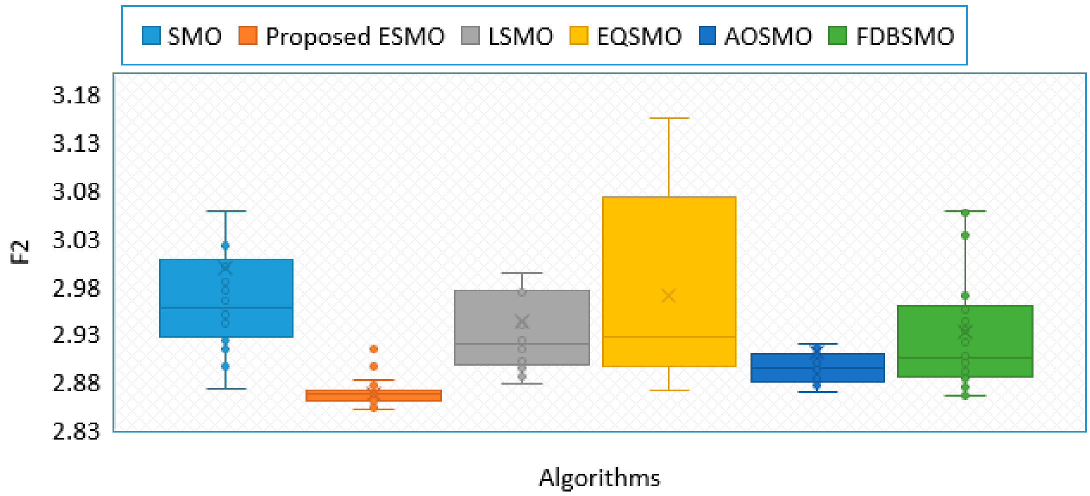

Figure 8. Box plot of the acquired losses via the proposed ESMO and other recent SMO versions.

As shown, the suggested ESMO was the most effective version at producing the lowest power losses. In terms of mean power losses, the suggested ESMO achieved a value of 2.8677 MW, whereas the SMO, LSMO, EQSMO, AOSMO, and FDBSMO obtained values of 2.99839, 2.942707, 2.970576, 2.910941, and 2.933065 MW, respectively. In terms of the maximum power losses, the suggested ESMO achieved a value of 2.914 MW, whereas the SMO, LSMO, EQSMO, AOSMO, and FDBSMO obtained values of 3.3243, 3.148561, 3.155098, 3.073784, and 3.118624 MW, respectively. Moreover, the ESMO provided the lowest STd of 0.01269 relative to 0.113264, 0.071125, 0.100712, 0.051942, and 0.069051 for the SMO, LSMO, EQSMO, AOSMO, and FDBSMO, respectively.

4.1.3. Minimization of the Total Producing Emissions

Nowadays, there is great interest in the production of pollutant gases all over the world. Thus, the OPF problem can be mathematically solved to minimize the total produced emissions ($F3$), as described in Equation (24):

$$F3 = \sum_{k=1}^{Ngen} \left(A_k Pgen_k^{\ 2} + B_k Pgen_k + C_k\right)/100 + D_k e^{E_k Pgen_k} \tag{24}$$

where A_k, B_k, C_k, D_k, and E_k are the atmospheric coefficients of the produced emissions of each generator k.

For minimizing the emissions, the proposed ESMO and SMO were used, and their attained outputs are displayed in Table 10.

Table 10. Optimal results of the proposed ESMO and other recent SMO versions for minimizing the emissions.

Variables	Initial	SMO	Proposed ESMO	LSMO	EQSMO	AOSMO	FDBSMO
Vgen $_1$	1.0500	1.1	1.1	1.1	1.1	1.1	1.1
Vgen $_2$	1.0400	1.096354	1.096357	1.097996578	1.096180409	1.098807122	1.096206734
Vgen $_5$	1.0100	1.079503	1.07941	1.081597125	1.079346054	1.082941938	1.078506486
Vgen $_8$	1.0100	1.08681	1.087166	1.091032082	1.085989926	1.09400001	1.087012582
Vgen $_{11}$	1.0500	1.099738	1.1	1.099085656	1.098269993	1.061797205	1.1
Vgen $_{13}$	1.0500	1.099207	1.099834	1.099950061	1.099485885	1.1	1.099966593
Ta $_{6–9}$	1.0780	1.015615	1.0526	1.032079855	1.023655322	1.0731266	1.019289849
Ta $_{6–10}$	1.0690	0.937388	0.916771	0.959351211	0.930001004	0.916026262	0.931165942
Ta $_{4–12}$	1.0320	0.999944	0.990658	0.98533689	0.990800687	0.993867339	1.020575999
Ta $_{28–27}$	1.0680	0.981544	0.98187	0.994597626	0.975205887	1.007583168	0.995172232
Qcap $_{10}$	0	0.000111	4.549616	1.927801467	1.797372234	4.782056182	2.358931836
Qcap $_{12}$	0	1.88548	4.9999	4.548228762	1.309795523	3.716423429	4.15318608
Qcap $_{15}$	0	3.020388	0.394847	4.804725694	1.050136129	1.255422697	4.866707435
Qcap $_{17}$	0	3.067737	0.776326	1.87954392	1.406471174	4.820877558	0.180389178
Qcap $_{20}$	0	3.655352	4.999903	1.041218586	4.984295346	4.91890748	1.612733824
Qcap $_{21}$	0	2.024077	4.629759	4.1317633	4.604957817	4.999765024	0.554657733
Qcap $_{23}$	0	2.303044	4.597308	4.763479851	5	1.04876913	3.612030106
Qcap $_{24}$	0	4.141412	4.884661	3.603719722	3.7248026	3.728962339	4.94272429
Qcap $_{29}$	0	2.648556	3.467423	4.636432124	0.477582774	4.938723233	1.611635229
Pgen $_1$	99.2400	63.9794	63.9824	63.93708603	63.90248253	63.93782153	64.09423067
Pgen $_2$	80	67.450805	67.4480204	67.52824811	67.53597051	67.54182947	67.36693912
Pgen $_5$	50	50	49.99984589	50	50	49.99957803	50
Pgen $_8$	20	35	34.99975216	35	35	35	34.99988911
Pgen $_{11}$	20	29.99976934	30	30	30	30	30
Pgen $_{13}$	20	40	40	39.9999523	40	40	40
F3	0.23909633	0.204700981	0.20469247	0.20470874	0.20470045	0.204713264	0.204707036

In addition, Figure 9 depicts the convergence characteristics of the suggested ESMO and other SMO versions. The proposed ESMO clearly beat the other SMO versions in terms of reducing the total producing emissions, as the proposed ESMO achieved the lowest value of 0.20469247 ton/h vs. 0.23909633 ton/h in the initial condition for the SMO, while the other SMO versions achieved 0.204700981, 0.20470874, 0.20470045, 0.204713264, and 0.204707036 ton/h using LSMO, EQSMO, AOSMO, and FDBSMO, respectively.

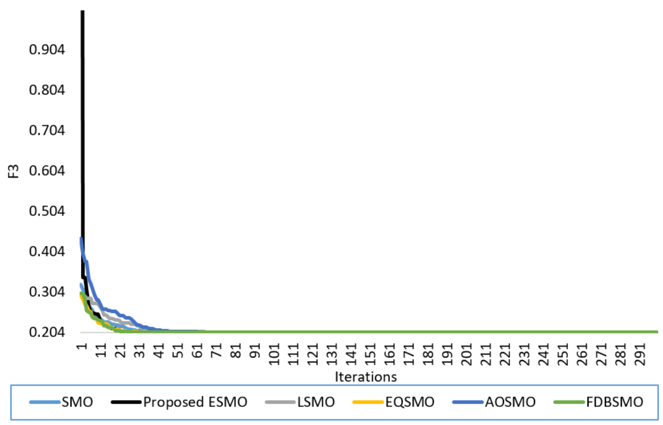

(**a**)

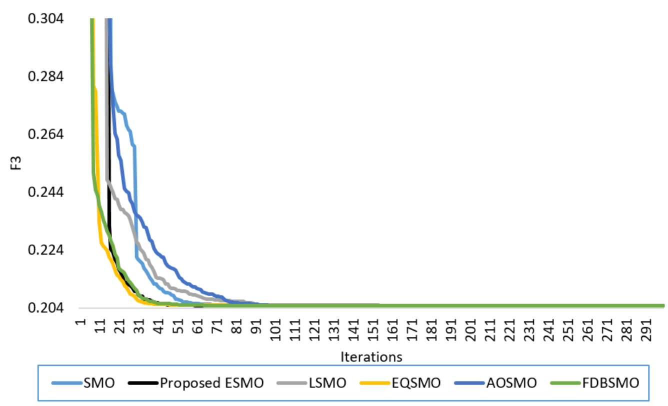

(**b**)

Figure 9. *Cont.*

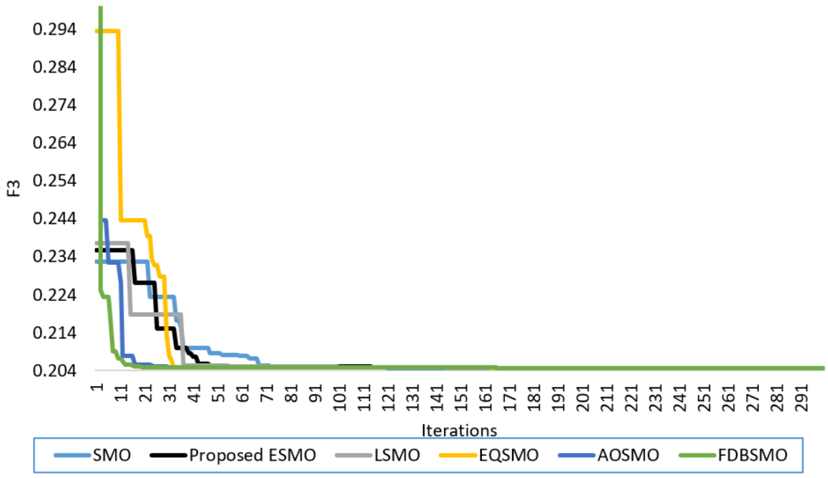

(**c**)

Figure 9. Convergences of the proposed ESMO and other recent SMO versions when minimizing the emissions. (**a**) Average convergence; (**b**) Median convergence; (**c**) Best convergence.

For this case, Table 11 shows a comparison with other meta-heuristics optimizers. As shown, the suggested ESMO attained the minimum emissions of 0.20469247 ton/h. It outperformed the other meta-heuristics of adaptive real coded biogeography-based optimization (ARBO) [64], Jaya algorithm [65], Stud Krill herd algorithm (KHA) [66], AGO [54], MCSO [49], KHA [66], GO [54], modified TLA [67], NBO [49], and CSO [49].

Table 11. Comparisons of the ESMO and other reported algorithms for minimizing the emissions.

Algorithm	F3
Proposed ESMO	0.20469247
SMO	0.204700981
Stud KHA [66]	0.2048
ARBO [64]	0.2048
Jaya [65]	0.204834
AGO [54]	0.20484
MCSO [49]	0.2048911
KHA [66]	0.2049
GO [54]	0.20492
Modified TLA [67]	0.20493
CSO [49]	0.2051355
NBO [49]	0.2052063

Additionally, after utilizing the suggested ESMO and other SMO versions, Figure 10 depicts the box plot of the thirty obtained fitnesses of the derived emissions. As shown, the suggested ESMO was effective at producing the lowest emissions. In terms of mean emissions, the suggested ESMO achieved a value of 0.20471 ton/h, whereas the SMO, LSMO, EQSMO, AOSMO, and FDBSMO obtained values of 0.20482, 0.204835, 0.204798, 0.204789, and 0.204778 ton/h, respectively. In terms of the maximum emissions, the suggested ESMO achieved a value of 0.204893 ton/h, whereas the SMO, LSMO, EQSMO, AOSMO, and FDBSMO obtained values of 0.204949, 0.204991, 0.204919, 0.204953, and 0.204862 ton/h, respectively. Furthermore, the ESMO provided the lowest STd of 3.54×10^{-5} relative to 8.12×10^{-5}, 8.56×10^{-5}, 7.14×10^{-5}, 7.18×10^{-5}, and 5.43×10^{-5} for the SMO, LSMO, EQSMO, AOSMO, and FDBSMO, respectively.

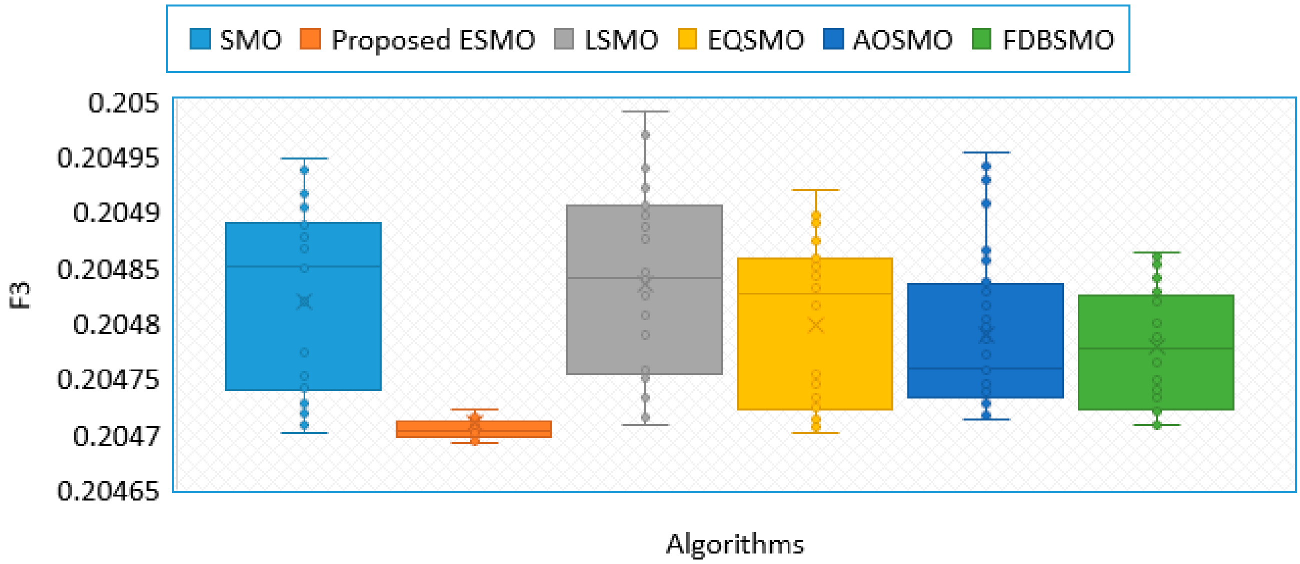

Figure 10. Box plot of the acquired emissions via the proposed ESMO and other recent SMO versions.

4.1.4. Wilcoxon Rank-Sum Test of the Implemented SMO Versions

In this part, the two-sided Wilcoxon rank-sum test was used, which is equivalent to a Mann–Whitney U-test, in order to return the *p*-values. The proposed ESMO was considered against each SMO version for the three cases studied and the test was executed. Table 12 displays the *p*-values that were found for each OPF fitness minimization. For the costs minimization, the majority of the *p*-values were less than 0.05, which indicated that the test rejected the null hypothesis at the default 5% significance level. For the losses minimization, the *p*-values, which were 7.39×10^{-11}, 2.37×10^{-10}, 3.82×10^{-10}, 5.0×10^{-9}, and 2.02×10^{-8} for SMO, LSMO, EQSMO, AOSMO, and FDBSMO, respectively, were less than 0.05. Similar findings were attained for the emissions minimization, where the *p*-values were 3.82×10^{-09}, 7.38×10^{-10}, 5.53×10^{-8}, 8.1×10^{-10}, and 1.43×10^{-8} for SMO, LSMO, EQSMO, AOSMO, and FDBSMO. Therefore, the Wilcoxon rank-sum test rejected the null hypothesis between the implemented SMO versions.

Table 12. Wilcoxon rank-sum test of the proposed ESMO against the other SMO versions.

Variables		SMO	LSMO	EQSMO	AOSMO	FDBSMO
p-value	Costs minimization	2.13×10^{-4}	5.6×10^{-7}	0.0251	0.0468	0.5997
	Losses minimization	7.39×10^{-11}	2.37×10^{-10}	3.82×10^{-10}	5.00×10^{-9}	2.02×10^{-8}
	Emissions minimization	3.82×10^{-9}	7.38×10^{-10}	5.53×10^{-8}	8.10×10^{-10}	1.43×10^{-8}

4.1.5. Evaluation of the Chaotic Strategy and Elitist Group with the ESMO

In this part, the two proposed differences in ESMO (chaotic strategy and elitist group) were evaluated independently and together in order to study the influence of those mechanisms on the behavior of the ESMO versus a standard SMO. The SMO with only the elitist group (SMO_Elitist), SMO with only the chaotic strategy (SMO_Chaotic), and the proposed ESMO, which involved both the chaotic strategy and elitist group, were assessed. For the three cases studied, SMO_Elitist, SMO_Chaotic, and the proposed ESMO were run with the same parameter settings that were previously defined in Table 6. Their obtained best, mean, worst, and STd values are recorded in Table 13. As shown, great enhancements are illustrated in the three cases studied, especially in the robustness behavior. For the costs minimization, the STd improvement was found to be 6.6379 and 74.9000% relative to SMO_Elitist and SMO_Chaotic, respectively. For the losses minimization, the STd improvement was found to be 87.4008 and 84.2415% relative to SMO_Elitist and SMO_Chaotic, respectively. For the emissions minimization, the STd improvement was found to be 50.4891 and 54.5761% relative to SMO_Elitist and SMO_Chaotic, respectively.

Table 13. Evaluation of the chaotic strategy and elitist group with the ESMO.

Case Study	Index	Proposed ESMO	SMO_Elitist	SMO_Chaotic
Costs minimization	Best	799.1133854	799.1730514	799.1932399
	Mean	799.248253	799.2955193	799.3774219
	Worst	799.4369998	799.4791913	799.694656
	STd	0.074834721	0.079802162	0.1308863
	STd improvement	-	6.6379%	74.9000%
Losses minimization	Index	Proposed ESMO	SMO_Elitist	SMO_Chaotic
	Best	2.852083219	2.870898634	2.876550431
	Mean	2.867769783	2.970575502	2.971105614
	Worst	2.914049709	3.155098093	3.18800886
	STd	0.012689716	0.100712161	0.080521342
	STd improvement	-	87.4008%	84.2415%
Emissions minimization	Index	Proposed ESMO	SMO_Elitist	SMO_Chaotic
	Best	0.20469247	0.20470045	0.204710214
	Mean	0.204710428	0.204798429	0.20481888
	Worst	0.204893097	0.204919011	0.204947592
	STd	3.53586×10^{-5}	7.14083×10^{-5}	7.78415×10^{-5}
	STd improvement	-	50.4891%	54.5761%

4.2. Optimal Combined Heat and Electrical Power Dispatch Problem

The combined heat and electrical power dispatch (CHEPD) problem was handled by considering a large-scale test case of 84 diverse units. The CHEPD's main purpose was to identify the best amount for heat and electrical power from heat-only generators, power-only generators, and co-generators in order to keep fuel prices low while meeting heat and electrical power needs and limitations exactly. Its objective was to minimize the system's total production costs. As a result, the generation cost reduction goal (F) may be expressed as:

$$F = \sum_{k=1}^{N_G} C_k(P_k) + \sum_{j=1}^{N_H} C_j(H_j) + \sum_{i=1}^{N_{CHP}} C_i(P_i, H_i) \tag{25}$$

where N_G, N_H, and N_{CHP} are the numbers of the power-only, heat-only, and co-generator units, respectively, while $C_k(P_k)$ [68], $C_j(H_j)$, and $C_i(P_i, H_i)$ are, respectively, the cost functions for the power-only, heat-only, and co-generator units, as follows:

$$C_k(P_k) = \alpha 1_k (P_k)^2 + \alpha 2_k P_k + \alpha 3_k + \left|\alpha 4_k \sin(\alpha 5_k (P_{k,\min} - P_k))\right| \tag{26}$$

$$C_j(H_j) = \varphi 1_j (H_j)^2 + \varphi 2_j H_j + \varphi 3_j \tag{27}$$

$$C_i(P_i, H_i) = \beta 1_i (P_i)^2 + \beta 2_i P_i + \beta 3_i + \beta 4_i (H_i)^2 + \beta 5_i H_i + \beta 6_i H_i P_i \tag{28}$$

where $\alpha 1$, $\alpha 2$, $\alpha 3$, $\alpha 4$, and $\alpha 5$ are the cost coefficients of the power units; $\varphi 1$, $\varphi 2$, and $\varphi 3$ are the cost coefficients of the heat units; and $\beta 1$, $\beta 2$, $\beta 3$, $\beta 4$, $\beta 5$, and $\beta 6$ are the cost coefficients for the co-generator units.

Added to this, inequality constraints of this issue must be satisfied in terms of the capacity of the power-only, heat-only, and co-generator units, as follows:

$$P_k^{\min} \le P_k \le P_k^{\max} \quad k = 1 : N_G \tag{29}$$

$$H_j^{\min} \le H_j \le H_j^{\max} \quad j = 1 : N_H \tag{30}$$

$$P_i^{\min} \le P_i \le P_i^{\max} \quad i = 1 : N_{CHP} \tag{31}$$

$$H_i^{\min} \le H_i \le H_i^{\max} \quad i = 1 : N_{CHP} \tag{32}$$

where the superscripts "min" and "max" indicate the minimum and maximum limits.

Moreover, equality constraints of this issue must be satisfied in terms of the power and heat balance, respectively, as follows:

$$\sum_{k=1}^{N_G} P_k + \sum_{i=1}^{N_{CHP}} P_i = P_{demand} \quad (33)$$

$$\sum_{j=1}^{N_H} H_j + \sum_{i=1}^{N_{CHP}} H_i = H_{demand} \quad (34)$$

where H_{demand} and P_{demand} are the system heat demand and electric demand, respectively.

For the CHEPD problem, a sizable case study with 84 different units was addressed. An electrical power load of 12,700 MW and a heat load of 5000 MWth were maintained for this system, which included twenty-four co-generation units, forty power-only units, and twenty heat-only units. Ref. [69] contains the complete data of the considered system and Table 14 tabulates the power and heat outputs from the power-only, heat-only, and co-generator units depending on the proposed ESMO and SMO algorithms. In addition, Figure 11 depicts the convergence characteristics of the suggested ESMO and SMO. The proposed ESMO clearly beat the SMO in terms of reducing the total production costs, as a lower fuel cost in the CHEPD system of USD 289,498.2 was obtained using the proposed ESMO compared to USD 290,362.8 using the conventional SMO.

Table 14. Results of the 84-unit CHEPD system from the production costs minimization using SMO and ESMO.

Unit	SMO	ESMO	Unit	SMO	ESMO	Unit	SMO	ESMO
P1	113.9974	73.44459	P38	109.9748	90.6213	H51	125.9833	107.7456
P2	74.05953	113.2413	P39	109.9961	109.9997	H52	113.3157	123.7505
P3	92.04989	99.33216	P40	511.3279	511.2792	H53	77.79472	77.54494
P4	133.6151	180.4777	P41	86.87628	108.6506	H54	116.0015	82.17562
P5	89.39002	94.273	P42	113.3483	152.9563	H55	96.60794	81.74176
P6	106.2412	107.4841	P43	116.9203	108.1153	H56	94.59446	82.75072
P7	261.9628	186.3668	P44	152.2478	123.2221	H57	42.32534	40.50032
P8	292.9954	297.196	P45	91.89126	92.14206	H58	44.5064	41.83042
P9	299.9997	287.3499	P46	41.66998	62.4102	H59	48.60778	47.76195
P10	204.7936	204.7983	P47	53.36528	74.27693	H60	47.00024	40.429
P11	243.5362	168.7863	P48	61.44711	80.61822	H61	41.26132	20.30929
P12	318.5471	318.4253	P49	107.9406	105.2862	H62	22.28054	30.79636
P13	304.6454	394.3084	P50	140.602	126.0701	H63	32.20353	20.44812
P14	304.6668	484.0242	P51	119.0138	86.26312	H64	22.91647	33.83084
P15	484.0212	484.0372	P52	96.18743	114.7725	H65	374.0721	385.4842
P16	483.8587	304.5231	P53	43.25877	42.94842	H66	372.5447	382.6649
P17	489.4774	489.294	P54	87.49657	48.31214	H67	375.9403	385.8598
P18	489.3831	489.3403	P55	65.05127	47.80923	H68	377.0608	382.8618
P19	511.3923	511.334	P56	62.70521	48.98129	H69	59.96803	59.99895
P20	512.2124	511.3195	P57	15.44486	11.2051	H70	60	59.99983
P21	530.2838	545.5427	P58	20.53013	14.27382	H71	59.99945	60
P22	532.1481	523.2856	P59	30.11782	28.11363	H72	59.99984	60
P23	523.3675	524.2476	P60	26.34874	11.00413	H73	59.99217	59.99981
P24	526.3741	523.6606	P61	81.77664	35.68019	H74	59.987	60
P25	523.7434	523.3108	P62	40.43841	58.77151	H75	60	59.99856
P26	523.3641	523.5737	P63	61.95136	36.01009	H76	60	59.99951
P27	10	10	P64	41.4247	65.42881	H77	120	120
P28	10.00883	10.00009	H41	108.0767	120.3123	H78	119.9998	119.9986
P29	10.00068	10	H42	122.9207	145.1812	H79	119.9982	119.9995
P30	96.97777	95.47952	H43	124.954	120.0116	H80	120	119.9997
P31	162.9052	189.9992	H44	144.741	128.4933	H81	120	120

Table 14. *Cont.*

Unit	SMO	ESMO	Unit	SMO	ESMO	Unit	SMO	ESMO
P32	189.9974	189.9996	H45	119.7918	120.0113	H82	119.9875	120
P33	162.2703	190	H46	76.44105	94.34085	H83	120	119.9995
P34	168.6657	171.2658	H47	86.52864	104.5896	H84	120	120
P35	199.9998	199.827	H48	93.48256	110.0641	Sum (Pg)	5000.0000	5000.0000
P36	168.4265	171.566	H49	119.885	118.4221	Sum (Hg)	12,700.0000	12,700.0000
P37	61.2683	103.6635	H50	138.2295	130.0936	F (USD)	290,362.8	289,498.2

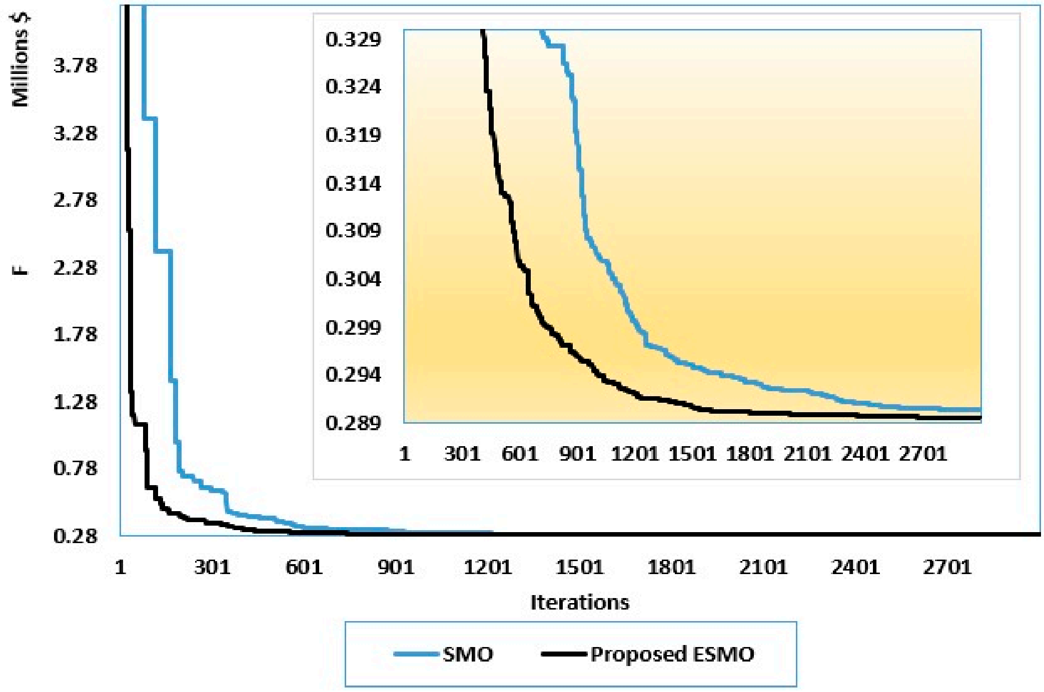

Figure 11. Convergences of the best obtained results using ESMO and SMO when minimizing the CHEPD production costs.

Table 15 contrasts the effectiveness of the suggested ESMO, which gave the optimal operating costs, with other current optimization methods, such as JFSO [70], WOA [69], MPA [71], IMPA [71], and the hybrid HT and JFSO (HT-JFSO) [70]. The suggested ESMO had the lowest costs and achieved the highest performance among the various optimizers, as shown in the table. This comparison validated the suggested ESMO's efficacy and superiority. Furthermore, Figure 12 depicts the box plot of the thirty obtained fitness of the derived production costs. As shown, the suggested ESMO was effective at producing lower fuel cost values. In terms of the mean fuel costs, the suggested ESMO achieved a value of 290,894.1 USD/h, whereas the SMO obtained a value of 291,812.6 USD/h. In terms of the maximum fuel costs, the suggested ESMO achieved a value of 293,371.5 USD/h, whereas the SMO obtained a value of 293,884.7 USD/h.

Table 15. Comparison of ESMO, SMO, and other reported techniques for the CHEPD problem.

Optimizer	F (USD)
Proposed ESMO	289,498.2
SMO	290,362.8
JFSO [70]	290,323.8
WOA [69]	290,123.97
MPA [71]	294,717.7
IMPA [71]	289,903.8

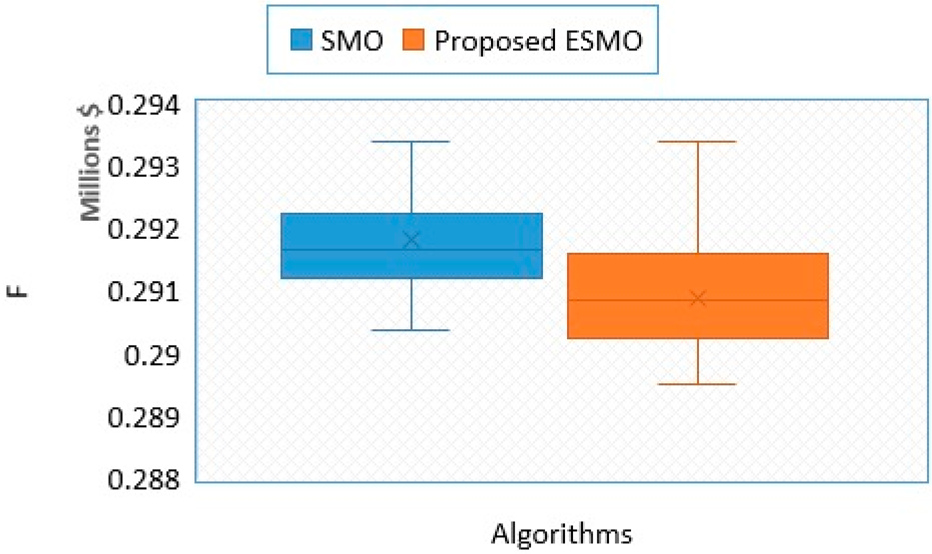

Figure 12. Box plot of the acquired CHEPD production costs via the proposed ESMO and SMO.

4.3. Friedman Ranking Test for Engineering Optimization Problems

Additionally, a Friedman ranking test of the best, mean, worst, and standard deviation obtained fitnesses was executed for the considered optimization cases of the OPF engineering problems for the suggested ESMO, SMO, LSMO, EQSMO, AOSMO, and FDBSMO, as depicted in Table 16. In this table, the great ability of the proposed ESMO at finding the first rank compared to the others is clearly shown.

Table 16. Friedman ranking test for OPF engineering problems.

Function	Index	Proposed ESMO	SMO	LSMO	EQSMO	AOSMO	FDBSMO
Costs minimization	Best	1	5	6	3	4	2
	Mean	2	5	6	4	3	1
	Worst	3	5	6	4	2	1
	STd	2	5	6	3	4	1
Losses minimization	Best	1	5	6	4	3	2
	Mean	1	6	4	5	2	3
	Worst	1	6	4	5	2	3
	STd	1	6	4	5	2	3
Emissions minimization	Best	1	3	5	2	6	4
	Mean	1	5	6	4	3	2
	Worst	2	4	6	3	5	1
	STd	1	5	6	3	4	2
Summation		17	60	65	45	40	25
Mean rank		1.416667	5	5.416667	3.75	3.333333	2.083333
Final ranking		1	5	6	4	3	2

4.4. Friedman and Post Hoc Tests for Engineering Optimization Problems

Moreover, Friedman and accompanying post hoc tests were implemented, where each method had a statistical distribution based on the outcome of its independent executions. For the OPF results, the related results are described in Table 17 by means of Friedman's ANOVA table in MATLAB. Moreover, the distribution of the outcomes for each case study is displayed in Appendix A. From this table, the null hypothesis was always rejected for all cases studied, where the probability of the p-value was always very small. For the first case regarding costs minimization, the recorded p-value was 9.5818×10^{-7}. For the second case regarding losses minimization, the recorded p-value was 3.65118×10^{-14}. For the third case regarding emissions minimization, the recorded p-value was 7.18362×10^{-12}.

Table 17. Friedman's ANOVA table (MATLAB) for the OPF results.

Case Study	Source	SS	df	MS	Chi-sq	Prob > Chi-sq
Costs minimization	Columns	125.933	5	25.1867	35.98	9.5818×10^{-7}
	Error	399.067	145	2.7522		
	Total	525	179			
Losses minimization	Columns	252.533	5	50.5067	72.15	3.6512×10^{-14}
	Error	272.467	145	1.8791		
	Total	525	179			
Emissions minimization	Columns	213.867	5	42.7733	61.1	7.1836×10^{-12}
	Error	311.133	145	2.1457		
	Total	525	179			

Added to this, the accompanying post hoc test is tabulated in Table 18. The second column shows the difference between the estimated group means (DGM). The first and third columns show the lower and upper limits for 95% confidence intervals for the true mean difference, which are addressed by "LCI" and "UCI", respectively. The last column containing the p-value for a hypothesis test shows that the corresponding mean difference was equal to zero. The majority of p-values were very small, which indicated that the proposed ESMO yield differed across all three minimization tasks.

Table 18. Post hoc test of the compared methods (MATLAB).

Costs Minimization				
Compared Methods	**LCI**	**DGM**	**UCI**	***p*-Value**
ESMO vs. SMO	−2.8432	−1.4667	−0.0901	0.0289
ESMO vs. LSMO	−3.6099	−2.2333	−0.8568	0.0001
ESMO vs. EQSMO	−2.3099	−0.9333	0.4432	0.3823
ESMO vs. AOSMO	−2.1765	−0.8	0.5765	0.561
ESMO vs. FDBSMO	−1.1432	0.2333	1.6099	0.9968
SMO vs. LSMO	−2.1432	−0.7667	0.6099	0.6071
SMO vs. EQSMO	−0.8432	0.5333	1.9099	0.8799
SMO vs. AOSMO	−0.7099	0.6667	2.0432	0.7391
SMO vs. FDBSMO	0.3235	1.7	3.0765	0.0058
LSMO vs. EQSMO	−0.0765	1.3	2.6765	0.0769
LSMO vs. AOSMO	0.0568	1.4333	2.8099	0.0356
LSMO vs. FDBSMO	1.0901	2.4667	3.8432	0
EQSMO vs. AOSMO	−1.2432	0.1333	1.5099	0.9998
EQSMO vs. FDBSMO	−0.2099	1.1667	2.5432	0.1508
AOSMO vs. FDBSMO	−0.3432	1.0333	2.4099	0.267
Losses Minimization				
Compared Methods	LCI	DGM	UCI	*p*-Value
ESMO vs. SMO	−5.1099	−3.7333	−2.3568	0
ESMO vs. LSMO	−4.1432	−2.7667	−1.3901	0
ESMO vs. EQSMO	−4.3432	−2.9667	−1.5901	0
ESMO vs. AOSMO	−3.1099	−1.7333	−0.3568	0.0045
ESMO vs. FDBSMO	−3.9765	−2.6	−1.2235	0
SMO vs. LSMO	−0.4099	0.9667	2.3432	0.3415
SMO vs. EQSMO	−0.6099	0.7667	2.1432	0.6071
SMO vs. AOSMO	0.6235	2	3.3765	0.0005
SMO vs. FDBSMO	−0.2432	1.1333	2.5099	0.1757
LSMO vs. EQSMO	−1.5765	−0.2	1.1765	0.9985
LSMO vs. AOSMO	−0.3432	1.0333	2.4099	0.267
LSMO vs. FDBSMO	−1.2099	0.1667	1.5432	0.9994
EQSMO vs. AOSMO	−0.1432	1.2333	2.6099	0.1091
EQSMO vs. FDBSMO	−1.0099	0.3667	1.7432	0.9742
AOSMO vs. FDBSMO	−2.2432	−0.8667	0.5099	0.4695

Table 18. *Cont.*

Emissions Minimization				
Compared Methods	LCI	DGM	UCI	p-Value
ESMO vs. SMO	1.7235	3.1	4.4765	0
ESMO vs. LSMO	−1.6099	−0.2333	1.1432	0.9968
ESMO vs. EQSMO	−0.7432	0.6333	2.0099	0.779
ESMO vs. AOSMO	−0.7765	0.6	1.9765	0.8161
ESMO vs. FDBSMO	−0.2765	1.1	2.4765	0.2033
SMO vs. LSMO	−4.7099	−3.3333	−1.9568	0
SMO vs. EQSMO	−3.8432	−2.4667	−1.0901	0
SMO vs. AOSMO	−3.8765	−2.5	−1.1235	0
SMO vs. FDBSMO	−3.3765	−2	−0.6235	0.0005
LSMO vs. EQSMO	−0.5099	0.8667	2.2432	0.4695
LSMO vs. AOSMO	−0.5432	0.8333	2.2099	0.515
LSMO vs. FDBSMO	−0.0432	1.3333	2.7099	0.064
EQSMO vs. AOSMO	−1.4099	−0.0333	1.3432	1
EQSMO vs. FDBSMO	−0.9099	0.4667	1.8432	0.9287
AOSMO vs. FDBSMO	−0.8765	0.5	1.8765	0.9062

In a similar manner, Friedman and accompanying post hoc tests were implemented described in Tables 19 and 20, respectively. Moreover, the distribution of the outcomes for each case study is displayed in Appendix A. From both tables, the null hypothesis was completely rejected, where the p-value based on Friedman's ANOVA and accompanied post hoc tests were 0.0003 and 0.000261, respectively.

Table 19. Friedman's ANOVA table (MATLAB) for the CHEPD results.

Case Study	**Source**	**SS**	**df**	**MS**	**Chi-sq**	**Prob > Chi-sq**
Costs minimization	Columns	6.66667	1	6.66667	13.33	0.0003
	Error	8.33333	29	0.28736		
	Total	15	59			

Table 20. Post hoc test of the compared methods (MATLAB) for the CHEPD results.

Costs Minimization				
Compared Methods	**LCI**	**DGM**	**UCI**	**p-Value**
ESMO vs. SMO	0.308831	0.666667	1.024502	0.000261

5. Conclusions

In the current study, an enhanced slime mould optimizer (ESMO) was proposed. The proposed ESMO was tested on 13 benchmark functions. In this study, the proposed ESMO incorporated a chaotic strategy and an elitist group to handle well-known engineering optimization problems called the optimal power flow and combined heat economic load dispatch. A chaotic strategy was integrated into the movement updating rule of the basic SMO, whereas the exploitation mechanism was enhanced via searching around an elitist group instead of only the global best dependence. To handle mathematical optimization problems, three cases were considered for the OPF problem. Applications were scrutinized on a typical IEEE test grid. The simulation results were compared with the results given in the former publications and were found to be competitive in terms of the quality of the solution. The second engineering application was the combined heat and electrical power dispatch problem, which was handled by considering a large-scale test case of 84 diverse units. Competitive findings were achieved using the suggested ESMO that surpassed the basic SMO and other recent techniques regarding minimizing the total production costs of heat and electrical energies. Moreover, the suggested ESMO outperformed the other optimization methods examined in terms of convergence rate, as well as solution merits. Furthermore, the statistical efficacy authenticated the quality of the suggested ESMO.

Considering the high efficacy of the suggested ESMO in the above-mentioned studies, it is mentioned that the proposed method should be tested for sufficiency when attempting to solve the OPF issue with the increasing penetration of renewable energies in electrical power networks in the future. It may also be designed for AC–DC power grids with the incorporation of modern voltage source converters. The limitation of the methodology adopted in this work, like the other meta-heuristic techniques, is a dependence on the parameter settings. Fortunately, only two parameter settings are required for the proposed ESMO, which are the numbers of individuals and iterations.

Author Contributions: Conceptualization, S.S., R.A.E.-S. and A.M.S.; methodology, A.M.S.; software, A.M.S.; validation, R.A.E.-S. and M.G.; formal analysis, A.M.S. and R.A.E.-S.; investigation, A.M.S. and M.G.; resources, M.G. and R.A.E.-S.; data curation, S.S.; writing—original draft preparation, S.S. and A.M.S.; writing—review and editing, R.A.E.-S.; visualization, M.G.; supervision, R.A.E.-S.; project administration, S.S.; funding acquisition, S.S. All authors have read and agreed to the published version of the manuscript.

Funding: The APC was funded by the Ministry of Education and King Abdulaziz University, Jeddah, Saudi Arabia.

Informed Consent Statement: Not applicable.

Data Availability Statement: Not applicable.

Acknowledgments: This research work was funded by Institutional Fund Projects under grant no.(IFPFP-263-22). Therefore, the authors gratefully acknowledge technical and financial' support from Ministry of Education and Deanship of Scientific Research (DSR), King Abdulaziz University (KAU), Jeddah, Saudi Arabia.

Conflicts of Interest: The authors declare no conflict of interest.

Appendix A

Table A1 describes the parameter settings of the implemented techniques related to Tables 3 and 4.

Table A1. Parameter settings of the implemented techniques.

Algorithm	Parameter Settings
ESMO	Adaptive parameters
SMO	Adaptive parameters
SCA	$A = 2$
SSA	$c_1 = c_2 \in [0, 1]$
WOA	$a_1 = [2, 0]$ $a_2 = [-2, -1]$ $b = 1$
MVO	travelling distance rate $\in [0.6, 1]$ existence probability $\in [0.2, 1]$
PSO	$c_1 = c_2 = 2$ $v_{Max} = 6$
DE	crossover probability = 0.5 scaling factor = 0.5

Figures A1–A3 show the distribution of the outcomes for each case study in the OPF problem for different objectives.

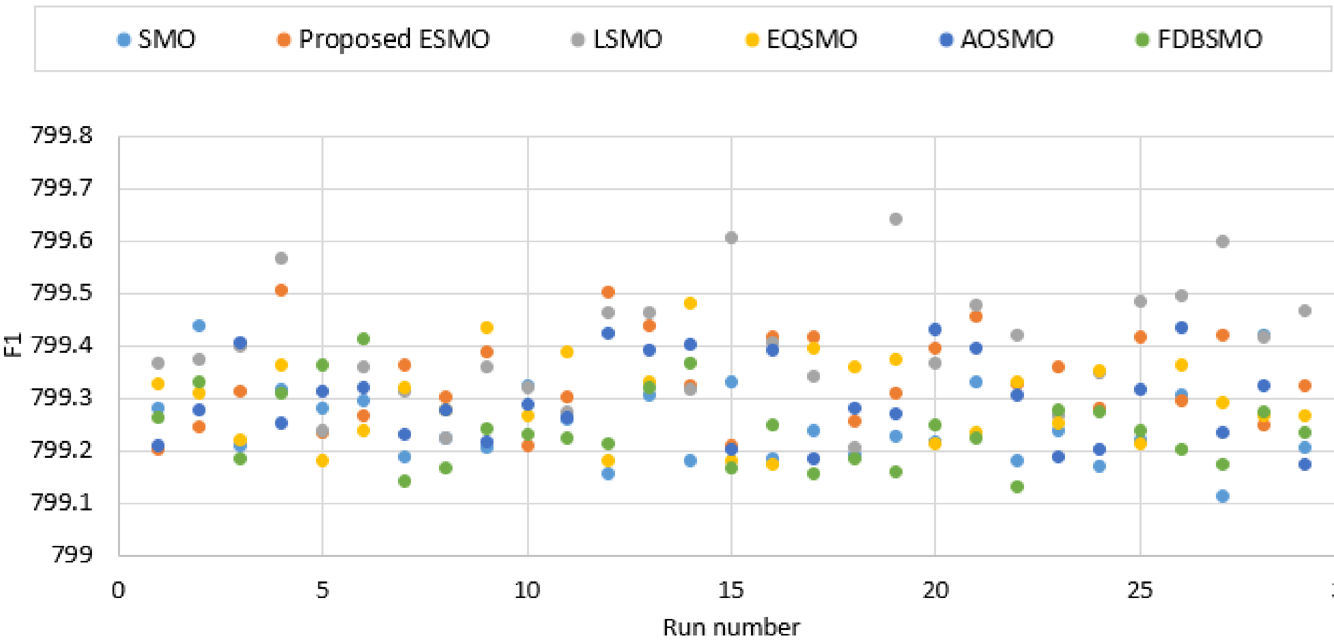

Figure A1. Distribution of the outcomes of the compared algorithms in order to minimize the costs in the OPF problem.

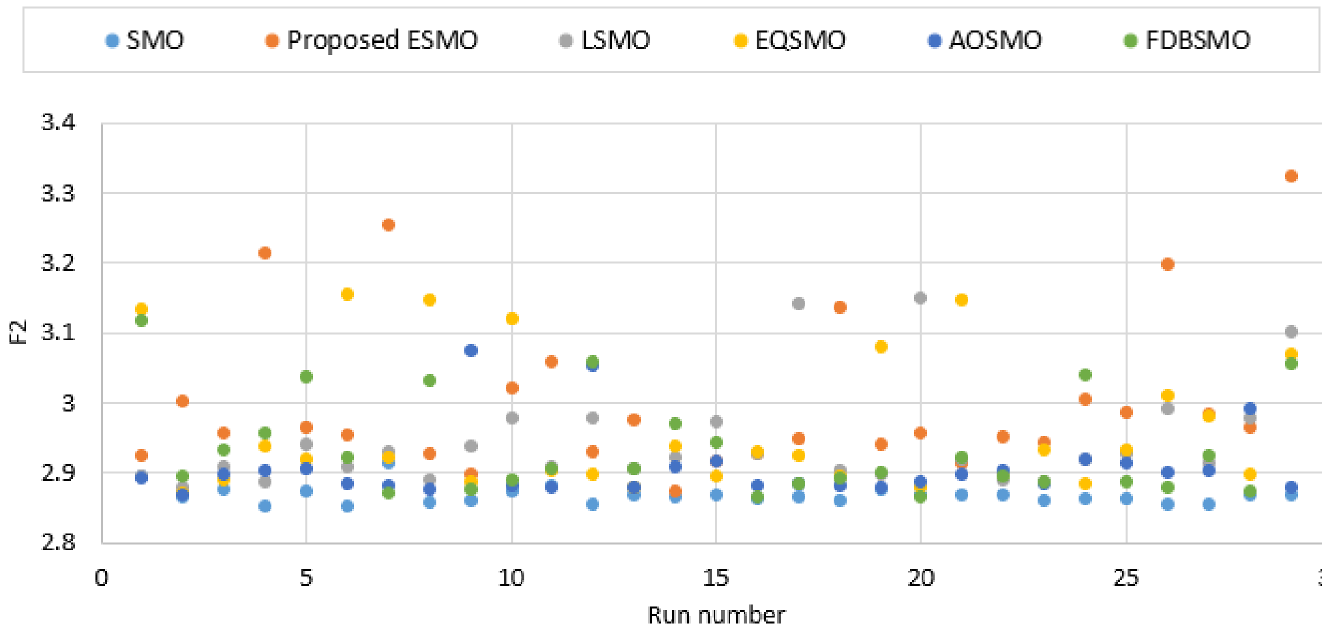

Figure A2. Distribution of the outcomes of the compared algorithms in order to minimize the losses in the OPF problem.

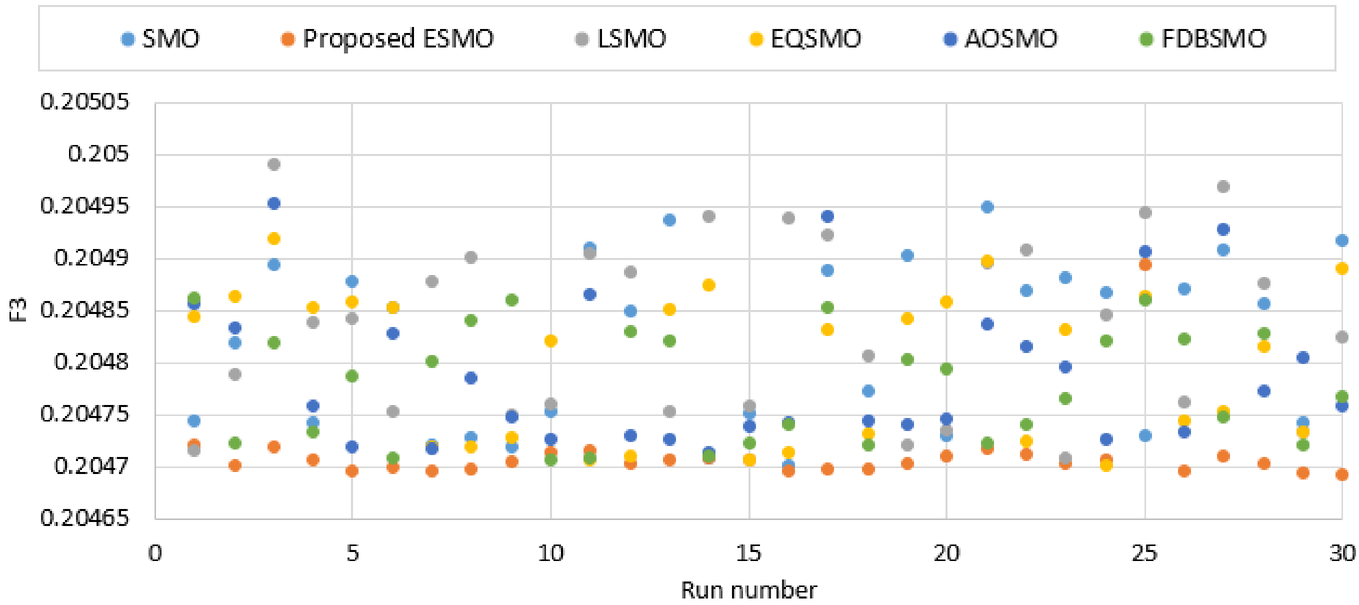

Figure A3. Distribution of the outcomes of the compared algorithms in order to minimize the emissions in the OPF problem.

References

1. Hajipour, V.; Kheirkhah, A.S.; Tavana, M.; Absi, N. Novel Pareto-based meta-heuristics for solving multi-objective multi-item capacitated lot-sizing problems. *Int. J. Adv. Manuf. Technol.* **2015**, *80*, 31–45. [CrossRef]
2. Hajipour, V.; Mehdizadeh, E.; Tavakkoli-Moghaddam, R. A novel Pareto-based multi-objective vibration damping optimization algorithm to solve multi-objective optimization problems. *Sci. Iran.* **2014**, *21*, 2368.
3. Wu, G. Across neighborhood search for numerical optimization. *Inf. Sci.* **2016**, *329*, 597–618. [CrossRef]
4. Hashim, F.A.; Houssein, E.H.; Mabrouk, M.S.; Al-Atabany, W.; Mirjalili, S. Henry gas solubility optimization: A novel physics-based algorithm. *Futur. Gener. Comput. Syst.* **2019**, *101*, 646–667. [CrossRef]
5. Shaheen, A.M.; Elattar, E.E.; El Sehiemy, R.A.; Elsayed, A.M. An Improved Sunflower Optimization Algorithm Based-Monte Carlo Simulation for Efficiency Improvement of Radial Distribution Systems Considering Wind Power Uncertainty. *IEEE Access* **2020**, *9*, 2332–2344. [CrossRef]
6. Bentouati, B.; Javaid, M.S.; Bouchekara, H.R.E.H.; El-Fergany, A.A. Optimizing performance attributes of electric power systems using chaotic salp swarm optimizer. *Int. J. Manag. Sci. Eng. Manag.* **2020**, *15*, 165–175. [CrossRef]
7. Li, S.; Gong, W.; Wang, L.; Yan, X.; Hu, C. Optimal power flow by means of improved adaptive differential evolution. *Energy* **2020**, *198*, 117314. [CrossRef]
8. Chen, X.; Li, K.; Xu, B.; Yang, Z. Biogeography-based learning particle swarm optimization for combined heat and power economic dispatch problem. *Knowl.-Based Syst.* **2020**, *208*, 106463. [CrossRef]
9. Abualigah, L.; Diabat, A.; Geem, Z.W. A comprehensive survey of the harmony search algorithm in clustering applications. *Appl. Sci.* **2020**, *10*, 3827. [CrossRef]
10. Faramarzi, A.; Heidarinejad, M.; Stephens, B.; Mirjalili, S. Equilibrium optimizer: A novel optimization algorithm. *Knowl.-Based Syst.* **2019**, *191*, 105190. [CrossRef]
11. Elgamal, Z.M.; Yasin, N.M.; Sabri, A.Q.M.; Sihwail, R.; Tubishat, M.; Jarrah, H. Improved equilibrium optimization algorithm using elite opposition-based learning and new local search strategy for feature selection in medical datasets. *Computation* **2021**, *9*, 68. [CrossRef]
12. Sun, F.; Yu, J.; Zhao, A.; Zhou, M. Optimizing multi-chiller dispatch in HVAC system using equilibrium optimization algorithm. *Energy Rep.* **2021**, *7*, 5997–6013. [CrossRef]
13. Lan, P.; Xia, K.; Pan, Y.; Fan, S. An improved equilibrium optimizer algorithm and its application in LSTM neural network. *Symmetry* **2021**, *13*, 1706. [CrossRef]
14. Goldberg, D.E. *Genetic Algorithms in Search, Optimization and Machine Learning*, 1989th ed.; Addison-Wesley Publishing Company, INC.: Redwood City, CA, USA, 1989.
15. Holland, J. *Adaptation in Natural and Artificial Systems: An Introductory Analysis with Applications to Biology, Control, and Artificial Intelligence*; MIT Press: Cambridge, MA, USA, 1992.
16. Das, D.B.; Patvardhan, C. A new hybrid evolutionary strategy for reactive power dispatch. *Electr. Power Syst. Res.* **2003**, *65*, 83–90.
17. Chou, J.S.; Truong, D.N. A novel metaheuristic optimizer inspired by behavior of jellyfish in ocean. *Appl. Math. Comput.* **2020**, *389*, 125535. [CrossRef]

18. Saremi, S.; Mirjalili, S.; Lewis, A. Grasshopper Optimisation Algorithm: Theory and application. *Adv. Eng. Softw.* **2017**, *105*, 30–47. [CrossRef]
19. Askari, Q.; Saeed, M.; Younas, I. Heap-based optimizer inspired by corporate rank hierarchy for global optimization. *Expert Syst. Appl.* **2020**, *161*, 113702. [CrossRef]
20. Mirjalili, S.; Lewis, A. The Whale Optimization Algorithm. *Adv. Eng. Softw.* **2016**, *95*, 51–67. [CrossRef]
21. Zhao, W.; Zhang, Z.; Wang, L. Manta ray foraging optimization: An effective bio-inspired optimizer for engineering applications. *Eng. Appl. Artif. Intell.* **2019**, *87*, 103300. [CrossRef]
22. Faramarzi, A.; Heidarinejad, M.; Mirjalili, S.; Gandomi, A.H. Marine predators algorithm: A nature-inspired Metaheuristic. *Expert Syst. Appl.* **2020**, *152*, 113377. [CrossRef]
23. Abou-El-Ela, A.A.; El-Sehiemy, R.A. Optimized generation costs using a modified particle swarm optimization version. In Proceedings of the 2008 12th International Middle East Power System Conference, MEPCON 2008, Aswan, Egypt, 12–15 March 2008; pp. 420–424. [CrossRef]
24. Karaboga, D.; Basturk, B. A powerful and efficient algorithm for numerical function optimization: Artificial bee colony (ABC) algorithm. *J. Glob. Optim.* **2007**, *39*, 459–471. [CrossRef]
25. Li, S.; Chen, H.; Wang, M.; Heidari, A.A.; Mirjalili, S. Slime mould algorithm: A new method for stochastic optimization. *Futur. Gener. Comput. Syst.* **2020**, *111*, 300–323. [CrossRef]
26. Hassan, M.H.; Kamel, S.; Abualigah, L.; Eid, A. Development and application of slime mould algorithm for optimal economic emission dispatch. *Expert Syst. Appl.* **2021**, *182*, 115205. [CrossRef]
27. Khunkitti, S.; Siritaratiwat, A.; Premrudeepreechacharn, S. Multi-objective optimal power flow problems based on slime mould algorithm. *Sustainability* **2021**, *13*, 7448. [CrossRef]
28. Nguyen, T.T.; Wang, H.J.; Dao, T.K.; Pan, J.S.; Liu, J.H.; Weng, S. An Improved Slime Mold Algorithm and its Application for Optimal Operation of Cascade Hydropower Stations. *IEEE Access* **2020**, *8*, 226754–226772. [CrossRef]
29. Yu, K.; Liu, L.; Chen, Z. An improved slime mould algorithm for demand estimation of urban water resources. *Mathematics* **2021**, *9*, 1316. [CrossRef]
30. Dhawale, D.; Kamboj, V.K.; Anand, P. An effective solution to numerical and multi-disciplinary design optimization problems using chaotic slime mold algorithm. *Eng. Comput.* **2021**. [CrossRef]
31. Naik, M.K.; Panda, R.; Abraham, A. Normalized square difference based multilevel thresholding technique for multispectral images using leader slime mould algorithm. *J. King Saud Univ.-Comput. Inf. Sci.* **2020**. [CrossRef]
32. Naik, M.K.; Panda, R.; Abraham, A. Adaptive opposition slime mould algorithm. *Soft Comput.* **2021**, *25*, 14297–14313. [CrossRef]
33. Naik, M.K.; Panda, R.; Abraham, A. An entropy minimization based multilevel colour thresholding technique for analysis of breast thermograms using equilibrium slime mould algorithm. *Appl. Soft Comput.* **2021**, *113*, 107955. [CrossRef]
34. Suiçmez, Ç.; Kahraman, H.; Yilmaz, C.; Işik, M.F.; Cengiz, E. Improved Slime-Mould-Algorithm with Fitness Distance Balance-based Guiding Mechanism for Global Optimization Problems. *Duzce Univ. J. Sci. Technol.* **2021**, *9*, 40–54. [CrossRef]
35. Eftimov, T.; Korošec, P.; Seljak, B.K. Disadvantages of Statistical Comparison of Stochastic Optimization Algorithms. In Proceedings of the 7th International Conference on Bioinspired Optimization Methods and their Applications, Bled, Slovenia, 18–20 May 2016.
36. Halim, A.H.; Ismail, I.; Das, S. Performance assessment of the metaheuristic optimization algorithms: An exhaustive review. *Artif. Intell. Rev.* **2020**, *54*, 2323–2409. [CrossRef]
37. Liu, M.; Li, Y.; Huo, Q.; Li, A.; Zhu, M.; Qu, N.; Chen, L.; Xia, M. A two-way parallel slime mold algorithm by flow and distance for the travelling salesman problem. *Appl. Sci.* **2020**, *10*, 6180. [CrossRef]
38. Premkumar, M.; Jangir, P.; Sowmya, R.; Alhelou, H.H.; Heidari, A.A.; Chen, H. MOSMA: Multi-Objective Slime Mould Algorithm Based on Elitist Non-Dominated Sorting. *IEEE Access* **2020**, *9*, 3229–3248. [CrossRef]
39. İzci, D.; Ekinci, S. Comparative performance analysis of slime mould algorithm for efficient design of proportional–integral–derivative controller. *Electrica* **2021**, *21*, 151–159. [CrossRef]
40. Kumari, S.; Chugh, R. A novel four-step feedback procedure for rapid control of chaotic behavior of the logistic map and unstable traffic on the road. *Chaos* **2020**, *30*, 123115. [CrossRef]
41. Mirjalili, S. SCA: A Sine Cosine Algorithm for solving optimization problems. *Knowl.-Based Syst.* **2016**, *96*, 120–133. [CrossRef]
42. Mirjalili, S.; Gandomi, A.H.; Mirjalili, S.Z.; Saremi, S.; Faris, H.; Mirjalili, S.M. Salp Swarm Algorithm: A bio-inspired optimizer for engineering design problems. *Adv. Eng. Softw.* **2017**, *114*, 163–191. [CrossRef]
43. Mirjalili, S.; Mirjalili, S.M.; Hatamlou, A. Multi-Verse Optimizer: A nature-inspired algorithm for global optimization. *Neural Comput. Appl.* **2015**, *27*, 495–513. [CrossRef]
44. Kennedy, J.; Eberhart, R. Particle Swarm Optimization. In Proceedings of the ICNN'95-International Conference on Neural Networks, Perth, Australia, 27 November–1 December 1995; IEEE: Washington, DC, USA, 1995.
45. Storn, R.; Price, K. Differential Evolution–A Simple and Efficient Heuristic for global Optimization over Continuous Spaces. *J. Glob. Optim.* **1997**, *11*, 341–359. [CrossRef]
46. Liu, Y.; Gong, D.; Sun, J.; Jin, Y. A Many-Objective Evolutionary Algorithm Using a One-by-One Selection Strategy. *IEEE Trans. Cybern.* **2017**, *47*, 2689–2702. [CrossRef] [PubMed]
47. El-Sehiemy, R.A.; El Ela, A.A.A.; Shaheen, A. A multi-objective fuzzy-based procedure for reactive power-based preventive emergency strategy. *Int. J. Eng. Res. Afr.* **2014**, *13*, 91–102. [CrossRef]

48. Shaheen, A.M.; El-Sehiemy, R.A. Application of Multi-Verse Optimizer for Transmission Network Expansion Planning in Power Systems. In Proceedings of the 2019 International Conference on Innovative Trends in Computer Engineering (ITCE), Aswan, Egypt, 2–4 February 2019.
49. Shaheen, A.M.; El-Sehiemy, R.A.; Elattar, E.E.; Abd-Elrazek, A.S. A Modified Crow Search Optimizer for Solving Non-Linear OPF Problem with Emissions. *IEEE Access* **2021**, *9*, 43107–43120. [CrossRef]
50. Jeddi, B.; Einaddin, A.H.; Kazemzadeh, R. A novel multi-objective approach based on improved electromagnetism-like algorithm to solve optimal power flow problem considering the detailed model of thermal generators. *Int. Trans. Electr. Energy Syst.* **2016**, *27*, e2293. [CrossRef]
51. Yang, X.S. Bat algorithm: Literature review and applications. *Int. J. Bio-Inspired Comput.* **2013**, *5*, 141–149. [CrossRef]
52. Askarzadeh, A. A novel metaheuristic method for solving constrained engineering optimization problems: Crow search algorithm. *Comput. Struct.* **2016**, *169*, 1–12. [CrossRef]
53. Bouchekara, H.R.E.H. Optimal power flow using black-hole-based optimization approach. *Appl. Soft Comput. J.* **2014**, *24*, 879–888. [CrossRef]
54. Alhejji, A.; Ebeed Hussein, M.; Kamel, S.; Alyami, S. Optimal Power Flow Solution with an Embedded Center-Node Unified Power Flow Controller Using an Adaptive Grasshopper Optimization Algorithm. *IEEE Access* **2020**, *8*, 119020–119037. [CrossRef]
55. Taher, M.A.; Kamel, S.; Jurado, F.; Ebeed, M. An improved moth-flame optimization algorithm for solving optimal power flow problem. *Int. Trans. Electr. Energy Syst.* **2019**, *29*, e2743. [CrossRef]
56. Ghasemi, M.; Ghavidel, S.; Gitizadeh, M.; Akbari, E. An improved teaching-learning-based optimization algorithm using Lévy mutation strategy for non-smooth optimal power flow. *Int. J. Electr. Power Energy Syst.* **2015**, *65*, 375–384. [CrossRef]
57. Abdo, M.; Kamel, S.; Ebeed, M.; Yu, J.; Jurado, F. Solving non-smooth optimal power flow problems using a developed grey wolf optimizer. *Energies* **2018**, *11*, 1692. [CrossRef]
58. Mohamed, A.A.A.; Mohamed, Y.S.; El-Gaafary, A.A.M.; Hemeida, A.M. Optimal power flow using moth swarm algorithm. *Electr. Power Syst. Res.* **2017**, *142*, 190–206. [CrossRef]
59. Duman, S. Symbiotic organisms search algorithm for optimal power flow problem based on valve-point effect and prohibited zones. *Neural Comput. Appl.* **2016**, *28*, 3571–3585. [CrossRef]
60. Ghanizadeh, A.J.; Mokhtari, M.; Abedi, M.; Gharehpetian, G.B. Optimal power flow based on imperialist competitive algorithm. *Int. Rev. Electr. Eng.* **2011**, *6*, 1847–1852.
61. Arul, R.; Ravi, G.; Velusami, S. Solving optimal power flow problems using chaotic self-adaptive differential harmony search algorithm. *Electr. Power Compon. Syst.* **2013**, *41*, 782–805. [CrossRef]
62. Zhang, J.; Wang, S.; Tang, Q.; Zhou, Y.; Zeng, T. An improved NSGA-III integrating adaptive elimination strategy to solution of many-objective optimal power flow problems. *Energy* **2019**, *172*, 945–957. [CrossRef]
63. Shaheen, A.; Ginidi, A.; El-Sehiemy, R.; Elsayed, A.; Elattar, E.; Dorrah, H.T. Developed Gorilla Troops Technique for Optimal Power Flow Problem in Electrical Power Systems. *Mathematics* **2022**, *10*, 1636. [CrossRef]
64. Ramesh Kumar, A.; Premalatha, L. Optimal power flow for a deregulated power system using adaptive real coded biogeography-based optimization. *Int. J. Electr. Power Energy Syst.* **2015**, *73*, 393–399. [CrossRef]
65. El-Sattar, S.A.; Kamel, S.; El Sehiemy, R.A.; Jurado, F.; Yu, J. Single- and multi-objective optimal power flow frameworks using Jaya optimization technique. *Neural Comput. Appl.* **2019**, *31*, 8787–8806. [CrossRef]
66. Pulluri, H.; Naresh, R.; Sharma, V. A solution network based on stud krill herd algorithm for optimal power flow problems. *Soft Comput.* **2018**, *22*, 159–176. [CrossRef]
67. Shabanpour-Haghighi, A.; Seifi, A.R.; Niknam, T. A modified teaching-learning based optimization for multi-objective optimal power flow problem. *Energy Convers. Manag.* **2014**, *77*, 597–607. [CrossRef]
68. Shaheen, A.M.; El-Sehiemy, R.A.; Elattar, E.; Ginidi, A.R. An Amalgamated Heap and Jellyfish Optimizer for economic dispatch in Combined heat and power systems including N-1 Unit outages. *Energy* **2022**, *246*, 123351. [CrossRef]
69. Nazari-Heris, M.; Mehdinejad, M.; Mohammadi-Ivatloo, B.; Babamalek-Gharehpetian, G. Combined heat and power economic dispatch problem solution by implementation of whale optimization method. *Neural Comput. Appl.* **2019**, *31*, 421–436. [CrossRef]
70. Ginidi, A.; Elsayed, A.; Shaheen, A.; Elattar, E.; El-Sehiemy, R. An Innovative Hybrid Heap-Based and Jellyfish Search Algorithm for Combined Heat and Power Economic Dispatch in Electrical Grids. *Mathematics* **2021**, *9*, 2053. [CrossRef]
71. Shaheen, A.M.; Elsayed, A.M.; Ginidi, A.R.; EL-Sehiemy, R.A.; Alharthi, M.M.; Ghoneim, S.S.M. A novel improved marine predators algorithm for combined heat and power economic dispatch problem. *Alex. Eng. J.* **2021**, *61*, 1834–1851. [CrossRef]